Master Thesis

Multi-Objective Optimization for Power Efficient Active IRS-Assisted Communication Systems

Dawei Shao

Institute for Digital Communications
Prof. Dr.-Ing. Robert Schober
University of Erlangen-Nuremberg

Supervisors: Prof. Dr.-Ing. Robert Schober
Dongfang Xu

March 9, 2022

Institute for Digital Communications

Prof. Dr.-Ing. Robert Schober
University of Erlangen-Nürnberg

Master Thesis

Multi-Objective Optimization for Power Efficient Active IRS-Assisted Communication Systems for Dawei Shao

Intelligent reflecting surfaces (IRSs) are emerging as promising enablers for the next generation of wireless communication systems, because of their ability to customize favorable radio propagation environments. However, with the conventional passive architecture, IRSs can only adjust the phase of the incident signals limiting the achievable beamforming gain. To fully unleash the potential of IRSs, a more general IRS architecture, i.e., active IRSs, has been proposed in recent works. In particular, equipped with reflection-type amplifiers, active IRSs can not only reflect the incident signals by manipulating the phase programmable IRS elements, but also amplify the reflected signal with the support of an extra power supply.

In practice, the total available power of communication systems is limited. On the other hand, to realize the potential gains facilitated by active IRSs, an appropriate amount of power has to be assigned to each element of the active IRS from the limited available power. As a result, compared to systems assisted by conventional passive IRSs, it is more important to smartly balance the base station (BS) transmit power and the IRS amplification power such that the quality-of-service (QoS) requirements of the users can be satisfied while guaranteeing power efficient communication. In this thesis, we consider an active IRS-assisted wireless communication system and investigate the power efficient resource allocation algorithm design for the considered communication system. The power efficient resource allocation design is formulated as a multi-objective optimization problem which jointly minimizes the BS transmit power and the amplification power at the active IRS. A corresponding optimization algorithm will be developed in the thesis.

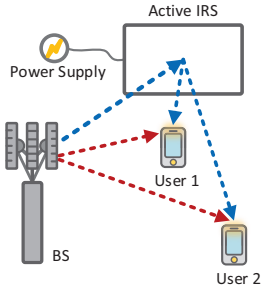

Figure 1: An active IRS-assisted multiuser communication system.

Main guidelines for the work:

- Acquisition of basic knowledge in communications and convex optimization theory
- Formulation of the optimization problem and development of a corresponding algorithm
- Verification of the adopted approach and presentation of results via simulation

---

SUPERVISORS Dongfang Xu {dongfang.xu@fau.de}

Student: Dawei Shao
Start date: Oct. 15, 2021

Prof. Dr.-Ing. Robert Schober
Lehrstuhl für Digitale Übertragung

Declaration

To the best of my knowledge and belief this work was prepared without aid from any other sources except where indicated. Any reference to material previously published by any other person has been duly acknowledged. This work contains no material which has been submitted or accepted for the award of any other degree in any institution.

Erlangen, March 9, 2022

Dawei Shao
Henkestrasse 43
Erlangen, Germany

Contents

Abstract

In this thesis, we investigate resource allocation algorithm design for multiuser Multiple-Input Single-Output (MISO) wireless communication systems. To enhance the system performance, an active Intelligent Reflecting Surface (IRS) is deployed in the considered system. Compared with the conventional passive IRS, active IRS can not only reflect the signal with the desired phase shift, but also amplify the reflected signal with the support of an extra power supply. Moreover, to guarantee secure communication, Artificial Noise (AN) is employed to deliberately impair the channels of the potential eavesdroppers. In practice, the total available power of communication systems is limited. To realize the potential gains facilitated by active IRS, an appropriate amount of power has to be assigned to active IRS. We exploit a multi-objective optimization framework to study two conflicting yet desirable design objectives, i.e., Base Station (BS) transmit power minimization and active IRS amplification power minimization. To this end, the weighed Tchebycheff method is adopted to formulate the resource allocation algorithm design as a multi-objective optimization problem. The considered multi-objective optimization problem takes into account the Quality-of-Service (QoS) of all legitimate users while guaranteeing secure transmission in the presence of potential eavesdroppers. Although the proposed multi-objective optimization problem is non-convex, we solve it optimally by employing Semidefinite Relaxation (SDR) and Inner Approximation (IA). Simulation results not only unveiled the trade-off in resource allocation between the BS and the active IRS, but also showed that the proposed scheme achieves considerable power savings compared to the baseline schemes.

Glossary

Abbreviations

AF	Amplify-and-Forward
AN	Artificial Noise
AO	Alternating Optimization
AWGN	Additive White Gaussian Noise
BS	Base Station
CSI	Channel State Information
DoFs	Degrees of Freedom
FD-AF	Full-duplex Amplifying and Forwarding
IRS	Intelligent Reflecting Surface
IA	Inner Approximation
KKT	Karush-Kuhn-Tucker
MISO	Multiple-Input Single-Output
MIMO	Multiple-Input Multiple-Output
MRT	Maximum Ratio Transmission
PHY	Physical Layer
QoS	Quality-of-Service
RF	Radio Frequency
SDR	Semidefinite Relaxation
SINR	Signal-to-Interference-plus-Noise Ratio
THz	Terahertz
UDNs	Ultra-Dense Networks

Operators

$\triangleq$	Defined as
$\exp(x)$	Exponent function of x
$\mathbb{C}$	The set of all complex numbers
$\mathbb{R}_{+}^{N\times 1}$	The set of all positive real-valued vectors
$\mathbb{C}^{N\times 1}$	The set of all complex-valued vectors
$\mathbb{C}^{N\times M}$	The set of all $N \times M$ complex-valued matrices
$\mathbb{H}^{N}$	The set of all $N \times N$ Hermitian matrices
$\mathbf{I}_N$	The $N \times N$ identity matrix
$x \in \mathscr{S}$	x is a member of the set $\mathscr{S}$
$\forall x$	Means that a statement holds for all x
$\mathbf{x}^H$	Conjugate transpose of $\mathbf{x}$
$\lvert x \rvert$	Absolute value of a complex scalar x

$\|\|\mathbf{x}\|\|$	Euclidean norm of a vector $\mathbf{x}$
$\mathrm{Tr}(\mathbf{X})$	Trace of matrix $\mathbf{X}$
$\mathrm{Rank}(\mathbf{X})$	Rank of matrix $\mathbf{X}$
$\|\mathbf{X}\|_F$	Frobenius norm of matrix $\mathbf{X}$
$\mathbf{X} \succeq 0$	Means matrix $\mathbf{X}$ is positive semidefinite
$\mathscr{E}\{x\}$	Statistical expectation of random variable x
$x \sim \mathscr{X}(\cdot)$	The random variable x has distribution $\mathscr{X}(\cdot)$
$\mathscr{CN}(\mu, \mathbf{R})$	The circularly symmetric complex Gaussian distribution with mean μ and covariance matrix $\mathbf{R}$
$\mathbf{x}^*$	The optimal value of variable $\mathbf{x}$
$\nabla_{\mathbf{x}} L(\mathbf{x})$	The gradient vector of function $L(\mathbf{x})$ with respect to $\mathbf{x}$

Symbols

b_k	Information symbol for user receiver k
$\mathbf{f}_k^H$	Channel vector for the reflection link between the active IRS and user k
$\mathbf{f}_i^H$	Channel vector for the reflection link between the active IRS and eavesdropper i
$\mathbf{F}$	Channel matrix between the BS and the IRS
$\mathbf{G}$	Channel matrix between the BS and the active IRS
Γ_k	Received SINR at user k
$\Gamma_{i,k}^{\mathrm{EVE}}$	Received SINR of eavesdropper i wiretapping user k
Γ_{req_k}	Minimum required SINR of user k
$\Gamma_{\mathrm{req}_{i,k}}^{\mathrm{EVE}}$	Maximum tolerant SINR of eavesdropper i wiretapping user k
$\mathbf{h}_k^H$	Channel vector for the direct link between the BS and user k
$\mathbf{h}_i^H$	Channel vector for the direct link between the BS and eavesdropper i
I	Number of potential eavesdroppers
K	Number of active users
M	Number of active IRS elements
N_{T}	Number of antennas at the BS
$\mathbf{P}$	Amplification factor matrix of the active IRS
r_k	Received signal at user k
r_i	Received signal at potential eavesdropper i
$\mathbf{\Theta}$	Phase shift matrix of the active IRS
ε	Tolerance factor of inner approximation algorithm
$\mathbf{w}_k$	Beamforming vector for user k
$\mathbf{W}_k$	Beamforming matrix for user k
$\mathbf{x}$	The transmit signal vector at the BS
$\mathbf{y}$	Reflected and amplified signal of the active IRS
$\mathbf{z}$	Artificial noise vector
$\mathbf{Z}$	Artificial noise covariance matrix

Chapter 1

Introduction

Over the past few decades, wireless communication has brought tremendous benefits to society. From 1G to 5G, with the development of technology, the system capacity has been significantly improved. Currently, researchers are working on the upcoming Beyond 5G and future 6G wireless networks with the commercialization of 5G communication networks around the world. Although some technologies such as Multiple-Input Multiple-Output (MIMO), Ultra-Dense Networks (UDNs), and Terahertz (THz) communication can significantly improve the wireless communication spectrum and energy efficiency [1], the high energy consumption and high hardware costs are still critical issues faced in practical implementations.

Recently, motivated by advances in meta-materials and electromagnetics, a revolutionary technique called IRS has be proposed to overcome above limitations [2]–[6]. Specifically, an IRS is a planar array which comprises a large number of low-cost passive reflecting elements. With the aid of a smart controller attached to the IRS, each element can reflect the incident signal with a desired phase shift [7]. By smartly manipulating the IRS elements, wireless channels can be proactively customized, which can significantly improve system performance [5]. In particular, the signals reflected by an IRS can add constructively or destructively with non-reflected signals to boost the desired signal power or suppress the co-channel interference, which enhances the communication performance without the need of deploying additional costly and energy-consuming communication infrastructures [8]. Compared to the conventional relaying concepts, where wireless signals are actively produced using costly Radio Frequency (RF) chains, IRSs only passively reflect signals that are already available in the network and do not require RF chains. Thus, IRSs are more economical and environmental friendly. Furthermore, IRSs can be flexibly integrated into existing wireless networks by deploying them on diverse structures, such as roadside billboards, building facades, windows, and even human clothes [6].

On the other hand, some works have proposed to deploy IRSs in wireless communication systems to improve system performance. In [9], [10] the authors developed a power-efficient resource allocation algorithm design for minimization of the total transmit power for an IRS-aided multiuser MISO system. In [11], the authors propose a robust resource allocation algorithm design for providing secure high-data rate communication for IRS-assisted wireless communication. The authors of [12] developed two computationally efficient algorithms for IRS-enabled multi-user wireless communication, which can achieve a higher spectral efficiency. The authors of [13] proposed a scalable optimization framework for large IRS-assisted SWIPT system. Thanks to its high array gain, high flexibility, low cost and low power [14], IRS is expected to improve channel capacity, extend coverage, and reduce power consumption for future 6G communications [15]–[17].

One of the most important advantages of IRS is the "square-law" array gain. Specifically, the array gain of N-element IRS is proportional to N^2 and is N times larger than that achievable with standard large-scale MIMO [3]. However, in practice, the conventional IRS with hundreds of passive elements can only achieve negligible capacity gains in the typical scenario where the direct link is not weak [18]. In contrast, significant capacity gains are only observed in atypical communication scenarios where the direct link between transmitter and receiver is completely blocked or very weak [15]–[17]. The reason for this phenomenon is the "double path loss" effect, i.e., the signal passing through the reflection link suffer from large-scale fading twice. Specifically, the equivalent path loss of the BS-IRS-receiver link is the product of the path losses of the BS-IRS link and IRS-receiver link, which is usually thousands of times larger than that of the direct link [18]. As a result, the "double path loss" effect makes the employment of passive IRSs in typical wireless environments inefficient in enhancing system performance. To compensate for the severe double path loss in the reflection link, one has to employ large passive IRS consisting of hundreds or even thousands of reflecting elements to achieve significant performance gains [18], [19]. However, deploying a large number of passive IRS elements significantly increases the complexity of channel estimation and IRS optimization [17], [20], which makes the design of IRS-assisted wireless systems challenging in practice. Hence, most existing works on IRS have bypassed this effect by only considering atypical scenarios with very poor direct links [15]–[17].

To overcome the above issues, the authors of [21] recently proposed the concept of active IRS. Different from conventional IRS, active IRS can not only reflect the signal with the desired phase shift, but also amplify the reflected signal with the support of an extra power supply. In particular, each element of the passive IRS consists of only an impedance adjustable circuit for phase shifting, while each element of the active IRS is

additionally equipped with an active reflection-type amplifier. It should be noted that the active IRS is fundamentally different from the Full-duplex Amplifying and Forwarding (FD-AF) relay in the hardware structure and transmission mode. Specifically, the conventional Amplify-and-Forward (AF) relay requires a power-consuming RF chain and orthogonal time/frequency resources to receive and transmit power amplified signals. This process introduces a delay caused by the signal processing at the relay. In contrast, the active IRS can instantaneously reflect and amplify signals with low-power reflection-type amplifiers, and the resulting delay between the direct link and the reflection link is negligible [20]. In [21], the authors investigated the joint transmit and reflect beamforming design for maximization of the system capacity of an active IRS-assisted multiuser communication system. In [21], the authors investigated the joint transmit and reflective beamforming design for system capacity maximization of active IRS-assisted multiuser communication systems and proposed a joint precoding algorithm to solve this problem. Extensive results showed that the existing passive IRS can only achieve negligible capacity gain of about 3% in the typical application scenario compared to a benchmark without IRS, while the proposed active IRS can achieve significant capacity gain of about 129%, thus overcoming the "double path loss" effect. The author of [22] studied the resource allocation algorithm design for an active IRS-assisted multiuser communication system. Simulation results unveil that deploying active IRS is a promising approach to enhance the system performance compared to conventional passive IRS, especially when strong direct links exist.

However, in practice, the total available power of a communication system is limited. To realize the potential gains facilitated by active IRS, an appropriate amount of power must be allocated to each element of the active IRS from the limited available power. As a result, compared to systems assisted by conventional passive IRSs, it is more important to smartly balance the BS transmit power and the active IRS amplification power while satisfying the QoS requirements of the users and guaranteeing power efficient communication. Therefore, there is a trade-off in resource allocation between BS and active IRS, which can be investigated under a multi-objective optimization framework. In the literature, multi-objective optimization is often adopted to study the trade-off between conflicting system design objectives via the concept of Pareto optimality. In [23], the authors investigated a power efficient resource allocation algorithm for full-duplex systems under a multi-objective optimization framework which unveiled a trade-off between total downlink and total uplink power consumption. Moreover, secrecy is also a critical concern for the design of practical wireless communication systems. The conventional approach for securing communications is to perform cryptographic encryption at the application layer [24], which may entail a relatively high complexity due to the

required key distribution and service management [25]. As a complement to cryptographic methods, Physical Layer (PHY)-security is an emerging technique to guarantee secure wireless communication in recent years [26]–[31]. In particular, BS equipped with multiple antennas can steer their beamforming vectors and inject AN to interfere the decoding process at the eavesdroppers [32]–[34]. In [35], the authors propose a thorough analysis and optimization framework for artificial noise assisted secure transmission in a MIMO wiretap channel. In [36], joint transmit signal and AN covariance matrix optimization was studied for secrecy rate maximization.

Motivated by the above discussion, in this thesis, we consider an active IRS-assisted wireless communication system and develop a robust resource allocation algorithm design. To guarantee communication security, we apply AN injection at BS to deliberately degrade the channels of the eavesdroppers. The power efficient resource allocation design for the considered system is formulated as a multi-objective optimization problem which jointly minimizes the BS transmit power and the active IRS amplification power. The proposed multi-objective optimization problem is formulated by adopting the weighted Tchebycheff method and solved optimally by employing SDR and IA. The resulting complete Pareto optimal set corresponds to a set of resource allocation policies. Thus, the operator can select a proper resource allocation policy from the set of available policies.

The rest of this paper is organized as follows. In Chapter 2, we present the considered active IRS-assisted communication system model. In Chapter 3, we introduce the adopted performance metrics for the considered system model and propose a multi-objective optimization problem to investigate the trade-off in resource allocation between the BS and active IRS. In Chapter 4, we first handle the coupling of the optimization variables and then recast the optimization problems into convex form. Simulation results and corresponding analysis are presented in Chapter 5 and the conclusion for the thesis is summarized in Chapter 6.

Chapter 2

Systems Model

In this chapter, we present the considered active IRS-assisted communication system model. Then, we describe the considered system in detail and express the transmit signal at the BS, the received signals at all the users and potential eavesdroppers, respectively.

We consider an active IRS-assisted MISO communication system, cf. Figure 2.1. In particular, the BS is equipped with $N_{\mathrm{T}} > 1$ antennas, indexed by $\mathcal{N} \triangleq \{1, \cdots, N_{\mathrm{T}}\}$, while all K legitimate users and I potential eavesdroppers are single-antenna devices. To help establish a favorable propagation environment for secure communication, an active IRS is deployed to assist information transmission from BS to users while impairing the channels of the potential eavesdroppers. In particular, the active IRS consists of M phase-shifting elements and each element is additionally equipped with an integrated active reflection-type amplifier supported by an extra power supply. Hence, each element of active IRS can not only smartly change the phase of the incident signal, but also amplify the reflected signal for effective beamforming. To simplify the notation, we define sets $\mathcal{M} = \{1, \cdots, M\}$, $\mathcal{K} = \{1, \cdots, K\}$, and $\mathcal{I} = \{1, \cdots, I\}$ to collect the indices of the acitve IRS elements, the legitimate users, and the potential eavesdroppers, respectively. Besides, to establish a performance upper bound for the considered system, we assume that the global Channel State Information (CSI) of all users and eavesdroppers is perfectly known at the BS for resource allocation.

The transmit signal at the BS is given by

$$\mathbf{x} = \sum_{k \in \mathcal{K}} \mathbf{w}_k b_k + \mathbf{z}, \tag{2.1}$$

where $\mathbf{w}_k \in \mathbb{C}^{N_{\mathrm{T}} \times 1}$ and $b_k \in \mathbb{C}$ denote the beamforming vector for the user k and the corresponding information bearing symbol. Without loss of generality, we assume $\mathcal{E}\left\{|b_k|^2\right\} = 1$, $\forall k \in \mathcal{K}$. To further enhance the PHY-security of the considered system, we adopt AN technique in this thesis. In particular, an AN, i.e., $\mathbf{z} \in \mathbb{C}^{N_{\mathrm{T}} \times 1}$, is generated by

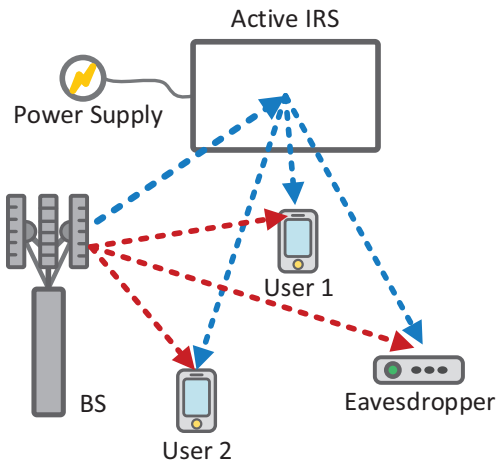

Figure 2.1: An active IRS-assisted multiuser communication system.

the BS to deliberately combat the channels of I potential eavesdroppers. Specifically, $\mathbf{z}$ is modelled as a complex Gaussian distribution with $\mathbf{z} \sim \mathscr{CN}(\mathbf{0}, \mathbf{Z})$, where $\mathbf{Z} \in \mathbb{H}^{N_T}$, $\mathbf{Z} \succeq \mathbf{0}$ is the covariance matrix of the AN. The artificial noise signal $\mathbf{z}$ is assumed unknown to both the users and the eavesdroppers.

With the reflection-type amplifier supported by a power supply, the reflected and amplified signal of an M-element active IRS can be modeled as follows

$$\mathbf{y} = \underbrace{\mathbf{P\Theta G x}}_{\text{Desired signal}} + \underbrace{\mathbf{P\Theta n_d}}_{\text{Dynamic noise}} + \underbrace{\mathbf{n_s}}_{\text{Static noise}}, \tag{2.2}$$

where $\mathbf{P} \triangleq \text{diag}(p_1, ..., p_M) \in \mathbb{R}_+^{M \times M}$ denotes the amplification factor matrix of the active IRS, where each element can be larger than one thanks to the integrated active amplifier. $\mathbf{\Theta} \triangleq \left(e^{j\theta_1}, ..., e^{j\theta_M}\right) \in \mathbb{C}^{M \times M}$ denotes the phase shift matrix of the active IRS. The channel between the BS and the active IRS is denoted by matrix $\mathbf{G} \in \mathbb{C}^{M \times N_T}$. Moreover, we note from (2.2) that the introduced noises can be divided into dynamic noise and static noise [21]. In particular, the the dynamic noise is generated due to the power amplification of active IRS [37], $\mathbf{n_d}$ is modelled as Additive White Gaussian Noise (AWGN), i.e.,$\mathbf{n_d} \sim \mathscr{CN}\left(\mathbf{0}_{N_T}, \sigma_d^2 \mathbf{I}_{N_T}\right)$. Furthermore, the static noise $\mathbf{n_s}$ is not affected by power amplification and is usually negligible compared with the dynamic noise $\mathbf{P\Theta n_d}$ [38]. Without loss of generality, we assume here $\mathbf{n_s} \sim \mathscr{CN}\left(\mathbf{0}_{N_T}, \sigma_s^2 \mathbf{I}_{N_T}\right)$.

The received signals at user k, eavesdropper i are given by, respectively,

$$r_k = \underbrace{\left(\mathbf{h}_k^H + \mathbf{f}_k^H \mathbf{P}\boldsymbol{\Theta}\mathbf{G}\right)\mathbf{w}_k b_k}_{\text{Desired signal}} + \underbrace{\left(\mathbf{h}_k^H + \mathbf{f}_k^H \mathbf{P}\boldsymbol{\Theta}\right)\sum_{r\in\mathscr{K}\setminus\{k\}} \mathbf{w}_r b_r}_{\text{Multiuser interference}}$$
$$+ \underbrace{\left(\mathbf{h}_k^H + \mathbf{f}_k^H \mathbf{P}\boldsymbol{\Theta}\mathbf{G}\right)\mathbf{z}}_{\text{Artificial noise}} + \underbrace{\mathbf{f}_k^H \mathbf{P}\boldsymbol{\Theta}\mathbf{n}_\mathbf{d}}_{\text{Dynamic noise introduced by active IRS}} + \underbrace{n_k}_{\text{Noise introduced at user } k}, \quad (2.3)$$

$$r_i = \left(\mathbf{h}_i^H + \mathbf{f}_i^H \mathbf{P}\boldsymbol{\Theta}\mathbf{G}\right)\left(\sum_{r\in\mathscr{K}} \mathbf{w}_k b_k + \mathbf{z}\right) + \mathbf{f}_i^H \mathbf{P}\boldsymbol{\Theta}\mathbf{n}_\mathbf{d} + n_i, \quad (2.4)$$

where $\mathbf{h}_k \in \mathbb{C}^{N_T \times 1}$ and $\mathbf{f}_k \in \mathbb{C}^{M\times 1}$ denote the channel vector between the BS and user k and the channel vector between the active IRS and user k, respectively. The channel vector between the BS and eavesdropper i and the channel vector between eavesdropper i and the active IRS are denoted by $\mathbf{h}_i \in \mathbb{C}^{N_\mathrm{T}\times 1}$ and $\mathbf{f}_i \in \mathbb{C}^{M\times 1}$, respectively. n_k and n_i denote the AWGN at user k and eavesdropper i, respectively. We assume here $n_k \sim \mathscr{CN}\left(0, \sigma_{n_k}^2\right)$ and $n_i \sim \mathscr{CN}\left(0, \sigma_{n_i}^2\right)$.

Chapter 3

Optimization Problems Formulation

In this chapter, we first define the adopted system performance metrics for the considered multiuser communication system. Then in Sections 3.2 and 3.3, we study the problem formulation of two desirable system design objectives for the considered active IRS-assisted communication system. Finally, we investigate these two system objectives jointly under the framework of multi-objective optimization in Section 3.4.

3.1 Performance Metrics

The received Signal-to-Interference-plus-Noise Ratio (SINR) at user k is given by

$$\Gamma_k = \frac{\left|\left(\mathbf{h}_k^H + \mathbf{f}_k^H \mathbf{P}\boldsymbol{\Theta}\mathbf{G}\right)\mathbf{w}_k\right|^2}{\sum\limits_{r\in\mathscr{K}\setminus\{k\}}\left|\left(\mathbf{h}_k^H + \mathbf{f}_k^H \mathbf{P}\boldsymbol{\Theta}\mathbf{G}\right)\mathbf{w}_r\right|^2 + \left|\left(\mathbf{h}_k^H + \mathbf{f}_k^H \mathbf{P}\boldsymbol{\Theta}\mathbf{G}\right)\mathbf{z}\right|^2 + \sigma_d^2\left\|\mathbf{f}_k^H \mathbf{P}\boldsymbol{\Theta}\right\|^2 + \sigma_{n_k}^2}. \tag{3.1}$$

On the other hand, the received SINR at eavesdropper i wiretapping user k, i.e., $\Gamma_{i,k}^{\mathrm{EVE}}$, is given by

$$\Gamma_{i,k}^{\mathrm{EVE}} = \frac{\left|\left(\mathbf{h}_i^H + \mathbf{f}_i^H \mathbf{P}\boldsymbol{\Theta}\mathbf{G}\right)\mathbf{w}_k\right|^2}{\sum\limits_{r\in\mathscr{K}\setminus\{k\}}\left|\left(\mathbf{h}_i^H + \mathbf{f}_i^H \mathbf{P}\boldsymbol{\Theta}\mathbf{G}\right)\mathbf{w}_r\right|^2 + \left|\left(\mathbf{h}_i^H + \mathbf{f}_i^H \mathbf{P}\boldsymbol{\Theta}\mathbf{G}\right)\mathbf{z}\right|^2 + \sigma_d^2\left\|\mathbf{f}_i^H \mathbf{P}\boldsymbol{\Theta}\right\|^2 + \sigma_{n_i}^2}. \tag{3.2}$$

3.2 Base Station Transmit Power Minimization

The first considered objective is designed to minimize the total BS transmit power which is comprised of the transmit signal power and the AN power while satisfying the QoS requirements of all users and guaranteeing the SINR of potential eavesdroppers

does not exceed the maximum tolerance. In particular, we focus on the following optimization problem

$$P_1: \underset{\mathbf{w}_k,\mathbf{P},\boldsymbol{\Theta},\mathbf{Z}\in\mathbb{H}^{N_T}}{\text{minimize}} \sum_{k\in\mathscr{K}} \|\mathbf{w}_k\|^2 + \text{Tr}(\mathbf{Z}) \tag{3.3}$$

$$\text{s.t. C1: } \frac{\left|\left(\mathbf{h}_k^H + \mathbf{f}_k^H\mathbf{P}\boldsymbol{\Theta}\mathbf{G}\right)\mathbf{w}_k\right|^2}{\sum_{r\in\mathscr{K}\setminus\{k\}}\left|\left(\mathbf{h}_k^H + \mathbf{f}_k^H\mathbf{P}\boldsymbol{\Theta}\mathbf{G}\right)\mathbf{w}_r\right|^2 + \left|\left(\mathbf{h}_k^H + \mathbf{f}_k^H\mathbf{P}\boldsymbol{\Theta}\mathbf{G}\right)\mathbf{z}\right|^2 + \sigma_d^2\left\|\mathbf{f}_k^H\mathbf{P}\boldsymbol{\Theta}\right\|^2 + \sigma_{n_k}^2} \geq \Gamma_{\text{req}_k},\ \forall k,$$

$$\text{C2: } \frac{\left|\left(\mathbf{h}_i^H + \mathbf{f}_i^H\mathbf{P}\boldsymbol{\Theta}\mathbf{G}\right)\mathbf{w}_k\right|^2}{\sum_{r\in\mathscr{K}\setminus\{k\}}\left|\left(\mathbf{h}_i^H + \mathbf{f}_i^H\mathbf{P}\boldsymbol{\Theta}\mathbf{G}\right)\mathbf{w}_r\right|^2 + \left|\left(\mathbf{h}_i^H + \mathbf{f}_i^H\mathbf{P}\boldsymbol{\Theta}\mathbf{G}\right)\mathbf{z}\right|^2 + \sigma_d^2\left\|\mathbf{f}_i^H\mathbf{P}\boldsymbol{\Theta}\right\|^2 + \sigma_{n_i}^2} \leq \Gamma_{\text{req}_{i,k}}^{\text{EVE}},\ \forall i,\ \forall k,$$

$$\text{C3: } \mathbf{Z}\succeq\mathbf{0}.$$

Here, Γ_{req_k} in constraint C1 is the minimum required SINR of user k. $\Gamma_{\text{req}_{i,k}}^{\text{EVE}}$ in constraint C2 indicates the maximum tolerant SINR of the potential eavesdropper i for wiretapping user k. Constraint C3 and $\mathbf{Z}\in\mathbb{H}^{N_T}$ are imposed since covariance matrix $\mathbf{Z}$ has to be a Hermitian positive semidefinite matrix. We note that the objective of Problem 1 is to minimize the total BS transmit power under constraints C1-C3 without regard for the amplification power consumed by the active IRS. Moreover, due to the highly coupled optimization variables, Problem 1 is non-convex.

In some papers [8], [21], such resource allocation optimization problems are usually solved by employing Alternating Optimization (AO)-based algorithms. However, by doing so, it destroys the joint optimality of the optimization variables. Moreover, it has been shown in [10] that the AO-based algorithms can converge to either the optimal solution or a large number of saddle points which may lead to unsatisfactory system performance. To preserve joint optimality, we employ an IA-based algorithm which is guaranteed to converge to a locally optimal solution of (3.3) [22]. The details of IA will be presented in Chapter 4.

3.3 Active IRS Amplification Power Minimization

For the second desirable system objective, we focus on minimizing the amplification power of active IRS under constraints C1-C3 without taking into account the BS transmit power. The optimization problem is formulated as follows

$$P_2: \quad \underset{\mathbf{w}_k,\mathbf{P},\boldsymbol{\Theta},\mathbf{Z}\in\mathbb{H}^{N_T}}{\text{minimize}} \sum_{k\in\mathscr{K}} \|\mathbf{P}\boldsymbol{\Theta}\mathbf{G}\mathbf{w}_k\|^2 + \sigma_d^2\|\mathbf{P}\boldsymbol{\Theta}\|^2 \tag{3.4}$$

$$\text{s.t. } \text{C1}: \Gamma_k \geq \Gamma_{\text{req}_k},\ \forall k,\ \ \text{C2}: \Gamma_{i,k}^{\text{EVE}} \leq \Gamma_{\text{req}_{i,k}}^{\text{EVE}},\ \forall k,\forall i$$

$$\text{C3: } \mathbf{Z}\succeq\mathbf{0}.$$

Due to the coupling of the optimization variables, the optimization problem in (3.4) is non-convex. Similarly, we apply the IA-based algorithm to obtain a locally optimal solution of (3.4).

3.4 Multi-Objective Optimization

The two above system design objectives are achievable for the BS and the active IRS, respectively. However, in practice, the total available power of communication systems is limited. On the other hand, to realize the potential gains facilitated by active IRS, an appropriate amount of power must be allocated to active IRS from the limited available power. Hence, there is a trade-off in resource allocation between BS and active IRS. Furthermore, it is important to smartly balance the BS transmit power and the active IRS amplification power while satisfying QoS requirements of the users and guaranteeing the secure communication.

To address above issue, we resort to multi-objective optimization. In the literature, multi-objective optimization is often adopted to investigate the trade-off between conflicting system design objectives via the concept of Pareto optimality [39],[40]. In the feasible objective space, a point is Pareto optimal if there is no other point that improves at least one of the objectives without degrade the others. In order to capture the complete Pareto optimal set, we formulate the third optimization problem to investigate the trade-off between Problem 1 and Problem 2 by using the weighted Tchebycheff method [29],[39]. The resulting problem formulation is given as:

$$P_3: \quad \underset{\mathbf{w}_k,\mathbf{P},\boldsymbol{\Theta},\mathbf{Z}\in\mathbb{H}^{N_T}}{\text{minimize}} \ \max_{i=1,2}\left\{\lambda_i\left(L_i - L_i^*\right)\right\} \quad \text{s.t.} \quad \text{C1}-\text{C3}, \tag{3.5}$$

where $L_1 = \sum_{k\in\mathcal{K}} \|\mathbf{w}_k\|^2 + \text{Tr}(\mathbf{Z})$ and $L_2 = \sum_{k\in\mathcal{K}} \|\mathbf{P}\boldsymbol{\Theta}\mathbf{G}\mathbf{w}_k\|^2 + \sigma_d^2 \|\mathbf{P}\boldsymbol{\Theta}\|^2$. L_i^* is the optimal objective value of the i-th problem. In particular, variable L_i^* is assumed to be a constant for resource allocation. The variable $\lambda_i \geq 0, \sum_i \lambda_i = 1$ is used to indicate the priority of the i-th objective compared to the other objectives, while reflecting the preference of the communication system designer. By varying λ_i, we can obtain the complete Pareto optimal set which corresponds to a set of resource allocation policies. As a result, we can select a proper resource allocation policy for communication system design from the set of available policies. Compared to other approaches for solving multi-objective optimization problems in the literature (e.g. the weighted product method, the exponentially weighted criterion, and the ϵ-constraint method [39]), the weighted Tchebycheff method can obtain the complete Pareto optimal set with a lower computational com-

plexity for convex and non-convex optimization problems . Furthermore, we note that Problem 3 is equivalent to Problem i when $\lambda_i = 1$ and $\lambda_j = 0 \ \forall i \neq j$, which means that both problem formulations have the same optimal solution.

Chapter 4

Solution of the Optimization Problems

In this chapter, in order to solve the above problems efficiently, we employ bilinear transformation and IA and develop a low-complexity iterative algorithm which is guaranteed to converge to locally optimal solutions of the optimization problems in (3.3) and (3.4) [22]. For the multi-objective optimization problem in (3.5), we employ the weighted Tchebycheff method to investigate the trade-off in resource allocartion between Problem 1 and Problem 2.

4.1 Bilinear Transformation

Since the matrices $\mathbf{P}$ and $\mathbf{\Theta}$ in (3.3) always appear in product form, we rewrite the product term $\mathbf{P\Theta}$ as $\mathbf{\Phi} = \text{diag}(p_1 e^{j\theta_1}, ..., p_M e^{j\theta_M})$. Then, the quadratic term $\sigma_d^2 \left\| \mathbf{f}_k^H \mathbf{P\Theta} \right\|^2$ in constaint C1 can be rewritten as follows

$$\sigma_d^2 \left\| \mathbf{f}_k^H \mathbf{P\Theta} \right\|^2 = \sigma_d^2 \text{Tr}\left(\mathbf{\Phi}^H \mathbf{F}_k \mathbf{\Phi} \right), \tag{4.1}$$

where $\mathbf{F}_k \in \mathbb{C}^{M \times M}$ is defined as $\mathbf{F}_k = \mathbf{f}_k \mathbf{f}_k^H$. To facilitate resource allocation algorithm design, we define $\mathbf{W}_k = \mathbf{w}_k \mathbf{w}_k^H, \ \forall k$, and rewrite the quadratic term $\left| \left(\mathbf{h}_k^H + \mathbf{f}_k^H \mathbf{\Phi G} \right) \mathbf{w}_r \right|^2$ in constraint C1 as:

$$\begin{aligned}
&\left| \left(\mathbf{h}_k^H + \mathbf{f}_k^H \mathbf{\Phi G} \right) \mathbf{w}_r \right|^2 \\
&= \mathbf{h}_k^H \mathbf{W}_r \mathbf{h}_k + \mathbf{f}_k^H \mathbf{\Phi G} \mathbf{W}_r \mathbf{G}^H \mathbf{\Phi}^H \mathbf{f}_k + 2\Re\left\{ \mathbf{h}_k^H \mathbf{W}_r \mathbf{G}^H \mathbf{\Phi}^H \mathbf{f}_k \right\} \\
&= \text{Tr}\left(\mathbf{H}_k \mathbf{W}_r \right) + \text{Tr}\left(\mathbf{\Phi G} \mathbf{W}_r \mathbf{G}^H \mathbf{\Phi}^H \mathbf{F}_k \right) \\
&+ \text{Tr}\left(\begin{bmatrix} \mathbf{f}_k \\ \mathbf{h}_k \end{bmatrix} \begin{bmatrix} \mathbf{f}_k^H & \mathbf{h}_k^H \end{bmatrix} \begin{bmatrix} \mathbf{0} & \mathbf{\Phi G} \mathbf{W}_r^H \\ \mathbf{W}_r \mathbf{G}^H \mathbf{\Phi}^H & \mathbf{0} \end{bmatrix} \right),
\end{aligned} \tag{4.2}$$

where $\mathbf{H}_k \in \mathbb{C}^{N_\mathrm{T}\times N_\mathrm{T}}$ is defined as $\mathbf{H}_k = \mathbf{h}_k\mathbf{h}_k^H$. Similarly, we rewrite the quadratic term $\left|\left(\mathbf{h}_k^H + \mathbf{f}_k^H\mathbf{P}\boldsymbol{\Theta}\mathbf{G}\right)\mathbf{z}\right|^2$ as:

$$\begin{aligned}
&\left|\left(\mathbf{h}_k^H + \mathbf{f}_k^H\boldsymbol{\Phi}\mathbf{G}\right)\mathbf{z}\right|^2 \\
&= \mathbf{h}_k^H\mathbf{Z}\mathbf{h}_k + \mathbf{f}_k^H\boldsymbol{\Phi}\mathbf{G}\mathbf{Z}\mathbf{G}^H\boldsymbol{\Phi}^H\mathbf{f}_k + 2\Re\left\{\mathbf{h}_k^H\mathbf{Z}\mathbf{G}^H\boldsymbol{\Phi}^H\mathbf{f}_k\right\} \\
&= \mathrm{Tr}\left(\mathbf{H}_k\mathbf{Z}\right) + \mathrm{Tr}\left(\boldsymbol{\Phi}\mathbf{G}\mathbf{Z}\mathbf{G}^H\boldsymbol{\Phi}^H\mathbf{F}_k\right) \\
&+\mathrm{Tr}\left(\begin{bmatrix}\mathbf{f}_k\\ \mathbf{h}_k\end{bmatrix}\begin{bmatrix}\mathbf{f}_k^H & \mathbf{h}_k^H\end{bmatrix}\begin{bmatrix}\mathbf{0} & \boldsymbol{\Phi}\mathbf{G}\mathbf{Z}^H\\ \mathbf{Z}\mathbf{G}^H\boldsymbol{\Phi}^H & \mathbf{0}\end{bmatrix}\right),
\end{aligned} \tag{4.3}$$

where $\mathbf{Z} \in \mathbb{H}^{N_\mathrm{T}}$, $\mathbf{Z} \succeq \mathbf{0}$ is the covariance matrix of the AN.

Then, the BS transmit power minimization problem in (3.3) can be equivalently reformulated as

$$\begin{aligned}
&\underset{\boldsymbol{\Phi},\mathbf{W}_k\in\mathbb{H}^{N_\mathrm{T}},\mathbf{Z}\in\mathbb{H}^{N_\mathrm{T}}}{\text{minimize}} \quad \sum_{k\in\mathscr{K}}\mathrm{Tr}\left(\mathbf{W}_k\right) + \mathrm{Tr}\left(\mathbf{Z}\right) \\
&\text{s.t.} \quad \text{C1: } \Gamma_k \geq \Gamma_{\mathrm{req}_k},\ \forall k, \quad \text{C2: } \Gamma_{i,k}^{\mathrm{EVE}} \leq \Gamma_{\mathrm{req}_{i,k}}^{\mathrm{EVE}},\ \forall k \\
&\qquad \text{C3: } \mathbf{Z} \succeq \mathbf{0},\ \text{C4: } \mathbf{W}_k \succeq \mathbf{0},\ \forall k,\ \text{C5: } \mathrm{Rank}\left(\mathbf{W}_k\right) \leq 1,\ \forall k.
\end{aligned} \tag{4.4}$$

On the other hand, we can recast the active IRS amplification power minimization problem in (3.4) as follows

$$\begin{aligned}
&\underset{\boldsymbol{\Phi},\mathbf{W}_k\in\mathbb{H}^{N_\mathrm{T}},\mathbf{Z}\in\mathbb{H}^{N_\mathrm{T}}}{\text{minimize}} \quad \sum_{k\in\mathscr{K}}\mathrm{Tr}\left(\boldsymbol{\Phi}\mathbf{G}\mathbf{W}_k\mathbf{G}^H\boldsymbol{\Phi}^H\right) + \sigma_d^2\mathrm{Tr}\left(\boldsymbol{\Phi}\boldsymbol{\Phi}^H\right) \\
&\text{s.t.} \quad \text{C1}: \Gamma_k \geq \Gamma_{\mathrm{req}_k},\ \forall k,\ \ \text{C2}: \Gamma_{i,k}^{\mathrm{EVE}} \leq \Gamma_{\mathrm{req}_{i,k}}^{\mathrm{EVE}},\ \forall k \\
&\qquad \text{C3: } \mathbf{Z} \succeq \mathbf{0},\ \text{C4: } \mathbf{W}_k \succeq \mathbf{0},\ \forall k,\ \text{C5: } \mathrm{Rank}\left(\mathbf{W}_k\right) \leq 1,\ \forall k.
\end{aligned} \tag{4.5}$$

We note that problems (4.4) and (4.5) are still non-convex due to the coupled $\mathbf{W}_k$ and $\boldsymbol{\Phi}$ involved in constraints C1 and C2 and the non-convex rank-one constraint C5. To overcome these obstacles, we take the term $\mathrm{Tr}\left(\boldsymbol{\Phi}\mathbf{G}\mathbf{W}_r\mathbf{G}^H\boldsymbol{\Phi}^H\mathbf{F}_k\right)$ in (4.2) as an example to interpret how to construct a convex approximation for the non-convex constraint C1. Before handling the highly-coupled non-convex constraint C1, we first have the following lemma.

Lemma 1: For any two Hermitian matrices $\mathbf{A} \in \mathbb{H}$ and $\mathbf{B} \in \mathbb{H}$ having the same size, we have the following two equalities:

$$\mathrm{Tr}\left(\mathbf{A}\mathbf{B}\right) = \frac{1}{2}\left\|\mathbf{A}+\mathbf{B}\right\|_F^2 - \frac{1}{2}\mathrm{Tr}\left(\mathbf{A}^H\mathbf{A}\right) - \frac{1}{2}\mathrm{Tr}\left(\mathbf{B}^H\mathbf{B}\right). \tag{4.6}$$

Proof: The right-hide side term of (4.6) can be rewritten as

$$\begin{aligned}
&\frac{1}{2}\|\mathbf{A}+\mathbf{B}\|_F^2-\frac{1}{2}\mathrm{Tr}\left(\mathbf{A}^H\mathbf{A}\right)-\frac{1}{2}\mathrm{Tr}\left(\mathbf{B}^H\mathbf{B}\right)\\
&=\frac{1}{2}\mathrm{Tr}\left((\mathbf{A}+\mathbf{B})^H(\mathbf{A}+\mathbf{B})\right)-\frac{1}{2}\mathrm{Tr}\left(\mathbf{A}^H\mathbf{A}\right)-\frac{1}{2}\mathrm{Tr}\left(\mathbf{B}^H\mathbf{B}\right)\\
&=\frac{1}{2}\mathrm{Tr}\left(\mathbf{A}^H\mathbf{A}\right)+\frac{1}{2}\mathrm{Tr}\left(\mathbf{A}^H\mathbf{B}\right)+\frac{1}{2}\mathrm{Tr}\left(\mathbf{B}^H\mathbf{A}\right)+\frac{1}{2}\mathrm{Tr}\left(\mathbf{B}^H\mathbf{B}\right)-\frac{1}{2}\mathrm{Tr}\left(\mathbf{A}^H\mathbf{A}\right)-\frac{1}{2}\mathrm{Tr}\left(\mathbf{B}^H\mathbf{B}\right)\\
&=\frac{1}{2}\mathrm{Tr}\left(\mathbf{A}^H\mathbf{B}\right)+\frac{1}{2}\mathrm{Tr}\left(\mathbf{B}^H\mathbf{A}\right)\overset{(a)}{=}\mathrm{Tr}\left(\mathbf{AB}\right)
\end{aligned}$$

where (a) is due to the fact that $\mathbf{A}$ and $\mathbf{B}$ are Hermitian matrices.

Based on ***Lemma 1***, the coupling term $\mathrm{Tr}\left(\mathbf{\Phi G W}_r\mathbf{G}^H\mathbf{\Phi}^H\mathbf{F}_k\right)$ in (4.2) can be rewritten as

$$\begin{aligned}
\mathrm{Tr}\left(\mathbf{\Phi G W}_r\mathbf{G}^H\mathbf{\Phi}^H\mathbf{F}_k\right)=&\frac{1}{2}\left\|\mathbf{\Phi}+\mathbf{G W}_r\mathbf{G}^H\mathbf{\Phi}^H\mathbf{F}_k\right\|_F^2-\frac{1}{2}\mathrm{Tr}\left(\mathbf{\Phi}^H\mathbf{\Phi}\right)\\
&-\frac{1}{2}\mathrm{Tr}\left(\mathbf{F}_k^H\mathbf{\Phi G W}_r^H\mathbf{G}^H\mathbf{G W}_r\mathbf{G}^H\mathbf{\Phi}^H\mathbf{F}_k\right).
\end{aligned}\tag{4.7}$$

We note that the right-hand side term of (4.7) is non-convex, since it contains bilinear functions of optimization variables $\mathbf{W}_r$ and $\mathbf{\Phi}$. To tackle this issue, we define a new optimization variable $\mathbf{U}_r=\mathbf{W}_r\mathbf{G}^H\mathbf{\Phi}^H$, where $\mathbf{U}_r\in\mathbb{C}^{N_\mathrm{T}\times M}$. Next, we transform $\mathbf{U}_r=\mathbf{W}_r\mathbf{G}^H\mathbf{\Phi}^H$ into a more tractable form by exploiting the following lemma.

Lemma 2: The equality constraint $\mathbf{U}_r=\mathbf{W}_r\mathbf{G}^H\mathbf{\Phi}^H$ is equivalent to the following inequalities constraints with the auxiliary variables $\mathbf{X}_r$ and $\mathbf{Y}_r$:

$$\text{C6:}\quad\begin{bmatrix}\mathbf{X}_r & \mathbf{U}_r & \mathbf{W}_r\mathbf{G}^H\\ \mathbf{U}_r^H & \mathbf{Y}_r & \mathbf{\Phi}\\ \mathbf{G W}_r^H & \mathbf{\Phi}^H & \mathbf{I}_M\end{bmatrix}\succeq\mathbf{0},\forall r\in\mathscr{K},\tag{4.8}$$

$$\text{C7:}\ \mathrm{Tr}\left(\mathbf{X}_r-\mathbf{W}_r\mathbf{G}^H\mathbf{G W}_r^H\right)\le 0,\forall r\in\mathscr{K}.\tag{4.9}$$

where $\mathbf{X}_r\in\mathbb{C}^{N_T\times N_T}$ and $\mathbf{Y}_r\in\mathbb{C}^{M\times M}$.

Proof: Before proving the Lemma 2, we first prove the following lemma [41].

Lemma 3: For given matrix $\overline{\mathbf{A}}$ and positive definite matrix $\overline{\mathbf{B}}$ of size $n\times m$ and $m\times m$, respectively, one has

$$\begin{bmatrix}\mathbf{0} & \overline{\mathbf{A}}\\ \overline{\mathbf{A}}^T & \overline{\mathbf{B}}\end{bmatrix}\succeq\mathbf{0},\tag{4.10}$$

if and only if $\overline{\mathbf{A}}=\mathbf{0}$.

Proof: If $\overline{\mathbf{A}} = \mathbf{0}$, since $\overline{\mathbf{B}}$ is positive definite, then (4.10) obviously holds. Next, we prove that if (4.10) holds, then $\overline{\mathbf{A}} = \mathbf{0}$. First, the block matrix in (4.10) is positive semidefinite implying that

$$2\mathbf{x}^T\overline{\mathbf{A}}\mathbf{y} + \mathbf{y}^T\overline{\mathbf{B}}\mathbf{y} \geq 0, \quad \forall \mathbf{x} \in \mathbb{R}^n, \forall \mathbf{y} \in \mathbb{R}^m. \tag{4.11}$$

Now, for $\overline{\mathbf{A}} = \mathbf{0}$, the block matrix in (4.10) is obviously positive semidefinite. Conversely, if $\overline{\mathbf{A}} \neq \mathbf{0}$, we can always find a $\mathbf{x}$ such that the block matrix is not positive semidefinite. Specifically, if there is $\overline{\mathrm{A}}_{ij} \neq 0$, we assume $\mathbf{x}$ such that $\mathrm{x}_k = 0$ for $k \neq i$ and $\mathbf{y}$ such that $\mathrm{y}_l = 0$ for $l \neq j$. Then (4.11) gives

$$2\overline{\mathrm{A}}_{ij}\mathrm{x}_i\mathrm{y}_j + \overline{\mathrm{B}}_{jj}\mathrm{y}_j^2 \geq 0, \quad \forall \left(\mathrm{x}_i, \mathrm{y}_j\right)^T \in \mathbb{R}^2. \tag{4.12}$$

However, for every $y_j \neq 0$, we can select $x_i = -\frac{\overline{\mathrm{B}}_{jj}+1}{2\overline{\mathrm{A}}_{ij}}\mathrm{y}_j$ which makes the left hand side of (4.12) negative. Hence, we can always construct cases for $\overline{\mathrm{A}}_{ij} \neq 0$ which violate the positive semidefinite condition. The proof of Lemma 3 is completed. □

Next, we present the proof of Lemma 2. By applying Schur's complement [42], constraint C6 in (4.8) is equivalent to

$$\begin{bmatrix} \mathbf{X}_r & \mathbf{U}_r \\ \mathbf{U}_r^H & \mathbf{Y}_r \end{bmatrix} - \begin{bmatrix} \mathbf{W}_r\mathbf{G}^H \\ \mathbf{\Phi} \end{bmatrix} \begin{bmatrix} \mathbf{G}\mathbf{W}_r^H & \mathbf{\Phi}^H \end{bmatrix} = \begin{bmatrix} \mathbf{X}_r - \mathbf{W}_r\mathbf{G}^H\mathbf{G}\mathbf{W}_r^H & \mathbf{U}_r - \mathbf{W}_r\mathbf{G}^H\mathbf{\Phi}^H \\ \mathbf{U}_r^H - \mathbf{\Phi}\mathbf{G}\mathbf{W}_r^H & \mathbf{Y}_r - \mathbf{\Phi}\mathbf{\Phi}^H \end{bmatrix} \succeq \mathbf{0}, \tag{4.13}$$

which implies that $\mathbf{X}_r - \mathbf{W}_r\mathbf{G}^H\mathbf{G}\mathbf{W}_r^H \succeq \mathbf{0}$. Combined with constraint C7 in (4.9), we can derive $\mathbf{X}_r - \mathbf{W}_r\mathbf{G}^H\mathbf{G}\mathbf{W}_r^H = \mathbf{0}$. Then, applying lemma 3 to (4.13) yields $\mathbf{U}_r = \mathbf{W}_r\mathbf{G}^H\mathbf{\Phi}^H$, which completes the proof of Lemma 2. □

4.2 Inner Approximation

Based on Lemma 2, the term $\mathrm{Tr}\left(\mathbf{\Phi}\mathbf{G}\mathbf{W}_r\mathbf{G}^H\mathbf{\Phi}^H\mathbf{F}_k\right)$ in (4.7) can be rewritten as follows

$$\mathrm{Tr}\left(\mathbf{\Phi}\mathbf{G}\mathbf{W}_r\mathbf{G}^H\mathbf{\Phi}^H\mathbf{F}_k\right) = \frac{1}{2}\left\|\mathbf{\Phi} + \mathbf{G}\mathbf{U}_r\mathbf{F}_k\right\|_F^2 - \frac{1}{2}\mathrm{Tr}\left(\mathbf{\Phi}^H\mathbf{\Phi}\right) - \frac{1}{2}\mathrm{Tr}\left(\mathbf{F}_k^H\mathbf{U}_r^H\mathbf{G}^H\mathbf{G}\mathbf{U}_r\mathbf{F}_k\right). \tag{4.14}$$

We note that the quadratics terms $\mathrm{Tr}\left(\mathbf{\Phi}^H\mathbf{\Phi}\right)$ and $\mathrm{Tr}\left(\mathbf{F}_k^H\mathbf{U}_r^H\mathbf{G}^H\mathbf{G}\mathbf{U}_r\mathbf{F}_k\right)$ in (4.14) are non-convex, which are obstacles for efficient algorithm design. To tackle this issue, we em-

ploy first-order Taylor approximation to handle the quadratic terms via the iterative IA approach [22]. In particular, we have

$$\mathrm{Tr}\left(\mathbf{\Phi}^H\mathbf{\Phi}\right) \geq \mathrm{Tr}\left(\left(2\mathbf{\Phi}^{(j)}\right)^H\mathbf{\Phi}\right) - \left\|\mathbf{\Phi}^{(j)}\right\|_F^2, \tag{4.15}$$

$$\mathrm{Tr}\left(\mathbf{F}_k^H\mathbf{U}_r^H\mathbf{G}^H\mathbf{G}\mathbf{U}_r\mathbf{F}_k\right) \geq \mathrm{Tr}\left(\left(2\mathbf{F}_k^H\mathbf{G}^H\mathbf{G}\mathbf{U}_r^{(j)}\mathbf{F}_k\right)^H\mathbf{U}_r\right) - \left\|\mathbf{G}\mathbf{U}_r^{(j)}\mathbf{F}_k\right\|_F^2, \tag{4.16}$$

where $\mathbf{\Phi}^{(j)}$ and $\mathbf{U}_r^{(j)}$ are the feasible solution obtained in the j-th iteration. Hence, we can construct a convex upper bound for the term $\left|\left(\mathbf{h}_k^H + \mathbf{f}_k^H\mathbf{\Phi}\mathbf{G}\right)\mathbf{w}_r\right|^2$ as follows

$$\begin{aligned}
&\left|\left(\mathbf{h}_k^H + \mathbf{f}_k^H\mathbf{\Phi}\mathbf{G}\right)\mathbf{w}_r\right|^2 \\
&= \mathrm{Tr}\left(\mathbf{H}_k\mathbf{W}_r\right) + \mathrm{Tr}\left(\mathbf{\Phi}\mathbf{G}\mathbf{W}_r\mathbf{G}^H\mathbf{\Phi}^H\mathbf{F}_k\right) \\
&+\mathrm{Tr}\left(\begin{bmatrix}\mathbf{f}_k\\ \mathbf{h}_k\end{bmatrix}\begin{bmatrix}\mathbf{f}_k^H & \mathbf{h}_k^H\end{bmatrix}\begin{bmatrix}\mathbf{0} & \mathbf{\Phi}\mathbf{G}\mathbf{W}_r^H\\ \mathbf{W}_r\mathbf{G}^H\mathbf{\Phi}^H & \mathbf{0}\end{bmatrix}\right) \\
&\leq \mathrm{Tr}\left(\mathbf{H}_k\mathbf{W}_r\right) + \frac{1}{2}\left\|\mathbf{\Phi} + \mathbf{G}\mathbf{U}_r\mathbf{F}_k\right\|_F^2 \\
&-\mathrm{Tr}\left(\left(\mathbf{\Phi}^{(j)}\right)^H\mathbf{\Phi}\right) + \frac{1}{2}\left\|\mathbf{\Phi}^{(j)}\right\|_F^2 + \frac{1}{2}\left\|\mathbf{G}\mathbf{U}_r^{(j)}\mathbf{F}_k\right\|_F^2 \\
&\quad -\mathrm{Tr}\left(\left(\mathbf{F}_k^H\mathbf{G}^H\mathbf{G}\mathbf{U}_r^{(j)}\mathbf{F}_k\right)^H\mathbf{U}_r\right) + \mathrm{Tr}\left(\begin{bmatrix}\mathbf{f}_k\\ \mathbf{h}_k\end{bmatrix}\begin{bmatrix}\mathbf{f}_k^H & \mathbf{h}_k^H\end{bmatrix}\begin{bmatrix}\mathbf{0} & \mathbf{U}_r^H\\ \mathbf{U}_r & \mathbf{0}\end{bmatrix}\right).
\end{aligned} \tag{4.17}$$

Similarly, $\left|\left(\mathbf{h}_k^H + \mathbf{f}_k^H\mathbf{\Phi}\mathbf{G}\right)\mathbf{z}\right|^2$ in constraint C1 can be rewritten as

$$\begin{aligned}
\left|\left(\mathbf{h}_k^H + \mathbf{f}_k^H\mathbf{\Phi}\mathbf{G}\right)\mathbf{z}\right|^2 &= \mathrm{Tr}\left(\mathbf{H}_k\mathbf{Z}\right) + \mathrm{Tr}\left(\mathbf{\Phi}\mathbf{G}\mathbf{Z}\mathbf{G}^H\mathbf{\Phi}^H\mathbf{F}_k\right) \\
&\quad +\mathrm{Tr}\left(\begin{bmatrix}\mathbf{f}_k\\ \mathbf{h}_k\end{bmatrix}\begin{bmatrix}\mathbf{f}_k^H & \mathbf{h}_k^H\end{bmatrix}\begin{bmatrix}\mathbf{0} & \mathbf{\Phi}\mathbf{G}\mathbf{Z}^H\\ \mathbf{Z}\mathbf{G}^H\mathbf{\Phi}^H & \mathbf{0}\end{bmatrix}\right).
\end{aligned} \tag{4.18}$$

Furthermore, the coupling term $\mathrm{Tr}\left(\mathbf{\Phi}\mathbf{G}\mathbf{Z}\mathbf{G}^H\mathbf{\Phi}^H\mathbf{F}_k\right)$ in (4.18) can be rewritten as

$$\begin{aligned}
\mathrm{Tr}\left(\mathbf{\Phi}\mathbf{G}\mathbf{Z}\mathbf{G}^H\mathbf{\Phi}^H\mathbf{F}_k\right) &= \frac{1}{2}\left\|\mathbf{\Phi} + \mathbf{G}\mathbf{Z}\mathbf{G}^H\mathbf{\Phi}^H\mathbf{F}_k\right\|_F^2 - \frac{1}{2}\mathrm{Tr}\left(\mathbf{\Phi}^H\mathbf{\Phi}\right) \\
&\quad -\frac{1}{2}\mathrm{Tr}\left(\mathbf{F}_k^H\mathbf{\Phi}\mathbf{G}\mathbf{Z}^H\mathbf{G}^H\mathbf{G}\mathbf{Z}\mathbf{G}^H\mathbf{\Phi}^H\mathbf{F}_k\right).
\end{aligned} \tag{4.19}$$

We note that the right-hand side term of (4.19) is non-convex, since it contains bilinear functions of optimization variables $\mathbf{Z}$ and $\mathbf{\Phi}$. Similarly, we define a new optimization

variable $\mathbf{Q} = \mathbf{Z}\mathbf{G}^H\mathbf{\Phi}^H$, where $\mathbf{Q} \in \mathbb{C}^{N_\mathrm{T}\times M}$. Based on Lemma 2, the equality constraint $\mathbf{Q} = \mathbf{Z}\mathbf{G}^H\mathbf{\Phi}^H$ can be transformed into the following inequalities constraints:

$$\text{C8: } \begin{bmatrix} \mathbf{M} & \mathbf{Q} & \mathbf{Z}\mathbf{G}^H \\ \mathbf{Q}^H & \mathbf{N} & \mathbf{\Phi} \\ \mathbf{G}\mathbf{Z}^H & \mathbf{\Phi}^H & \mathbf{I}_M \end{bmatrix} \succeq \mathbf{0}, \tag{4.20}$$

$$\text{C9: } \mathrm{Tr}\left(\mathbf{M} - \mathbf{Z}\mathbf{G}^H\mathbf{G}\mathbf{Z}^H\right) \leq 0, \tag{4.21}$$

where $\mathbf{M} \in \mathbb{C}^{N_T\times N_T}$ and $\mathbf{N} \in \mathbb{C}^{M\times M}$ are auxiliary variables. Then, we construct the convex upper bound for the term $\left|\left(\mathbf{h}_k^H + \mathbf{f}_k^H\mathbf{\Phi}\mathbf{G}\right)\mathbf{z}\right|^2$ as follows

$$\begin{aligned} &\left|\left(\mathbf{h}_k^H + \mathbf{f}_k^H\mathbf{\Phi}\mathbf{G}\right)\mathbf{z}\right|^2 \\ &\leq \mathrm{Tr}\left(\mathbf{H}_k\mathbf{Z}\right) + \frac{1}{2}\left\|\mathbf{\Phi} + \mathbf{G}\mathbf{Q}\mathbf{F}_k\right\|_F^2 - \mathrm{Tr}\left(\left(\mathbf{\Phi}^{(j)}\right)^H\mathbf{\Phi}\right) + \frac{1}{2}\left\|\mathbf{\Phi}^{(j)}\right\|_F^2 + \frac{1}{2}\left\|\mathbf{G}\mathbf{Q}^{(j)}\mathbf{F}_k\right\|_F^2 \\ &-\mathrm{Tr}\left(\left(\mathbf{F}_k^H\mathbf{G}^H\mathbf{G}\mathbf{Q}^{(j)}\mathbf{F}_k\right)^H\mathbf{Q}\right) + \mathrm{Tr}\left(\begin{bmatrix}\mathbf{f}_k \\ \mathbf{h}_k\end{bmatrix}\begin{bmatrix}\mathbf{f}_k^H & \mathbf{h}_k^H\end{bmatrix}\begin{bmatrix}\mathbf{0} & \mathbf{Q}^H \\ \mathbf{Q} & \mathbf{0}\end{bmatrix}\right). \end{aligned} \tag{4.22}$$

As a result, constraint C1 can be approximated by following convex constraint:

$$\begin{aligned} \widehat{\text{C1}}: &\Gamma_{\mathrm{req}_k}\left(\sum_{r\in\mathscr{K}\setminus\{k\}}\mathrm{Tr}\left(\mathbf{H}_k\mathbf{W}_r\right) + \mathrm{Tr}\left(\mathbf{H}_k\mathbf{Z}\right) + \sigma_d^2\mathrm{Tr}\left(\mathbf{\Phi}^H\mathbf{F}_k\mathbf{\Phi}\right) + \sigma_{n_k}^2\right) - \mathrm{Tr}\left(\mathbf{H}_k\mathbf{W}_k\right) \\ &+\frac{\Gamma_{\mathrm{req}_k}}{2}\sum_{r\in\mathscr{K}\setminus\{k\}}\left\|\mathbf{\Phi} + \mathbf{G}\mathbf{U}_r\mathbf{F}_k\right\|_F^2 - \left[K\Gamma_{\mathrm{req}_k} - 1\right]\left[\mathrm{Tr}\left(\left(\mathbf{\Phi}^{(j)}\right)^H\mathbf{\Phi}\right) - \frac{1}{2}\left\|\mathbf{\Phi}^{(j)}\right\|_F^2\right] \\ &-\Gamma_{\mathrm{req}_k}\sum_{r\in\mathscr{K}\setminus\{k\}}\left[\mathrm{Tr}\left(\left(\mathbf{F}_k^H\mathbf{G}^H\mathbf{G}\mathbf{U}_r^{(j)}\mathbf{F}_k\right)^H\mathbf{U}_r\right) - \frac{1}{2}\left\|\mathbf{G}\mathbf{U}_r^{(j)}\mathbf{F}_k\right\|_F^2\right] \\ &+\frac{\Gamma_{\mathrm{req}_k}}{2}\left\|\mathbf{\Phi} + \mathbf{G}\mathbf{Q}\mathbf{F}_k\right\|_F^2 - \Gamma_{\mathrm{req}_k}\left[\mathrm{Tr}\left(\left(\mathbf{F}_k^H\mathbf{G}^H\mathbf{G}\mathbf{Q}^{(j)}\mathbf{F}_k\right)^H\mathbf{Q}\right) - \frac{1}{2}\left\|\mathbf{G}\mathbf{Q}^{(j)}\mathbf{F}_k\right\|_F^2\right] \\ &-\frac{1}{2}\left\|\mathbf{\Phi} + \mathbf{G}\mathbf{U}_k\mathbf{F}_k\right\|_F^2 + \mathrm{Tr}\left(\left(\mathbf{F}_k^H\mathbf{G}^H\mathbf{G}\mathbf{U}_k^{(j)}\mathbf{F}_k\right)^H\mathbf{U}_k\right) - \frac{1}{2}\left\|\mathbf{G}\mathbf{U}_k^{(j)}\mathbf{F}_k\right\|_F^2 \\ &+\mathrm{Tr}\left(\mathbf{v}_k\mathbf{v}_k^H\begin{bmatrix}\mathbf{0} & \Gamma_{\mathrm{req}_k}\left(\sum_{r\in\mathscr{K}\setminus\{k\}}\mathbf{U}_r^H + \mathbf{Q}^H\right) - \mathbf{U}_k^H \\ \Gamma_{\mathrm{req}_k}\left(\sum_{r\in\mathscr{K}\setminus\{k\}}\mathbf{U}_r + \mathbf{Q}\right) - \mathbf{U}_k & \mathbf{0}\end{bmatrix}\right) \leq 0, \forall k, \end{aligned} \tag{4.23}$$

where $\mathbf{v}_k^H \in \mathbb{C}^{1\times(M+N_\mathrm{T})}$ is defined as $\mathbf{v}_k^H = \begin{bmatrix}\mathbf{f}_k^H & \mathbf{h}_k^H\end{bmatrix}$.

Similarly, constraint C2 can be approximated by the following constraint:

$$\begin{aligned}
\widehat{\mathrm{C2}}:\ & \mathrm{Tr}\left(\mathbf{H}_i\mathbf{W}_k\right)+\frac{1}{2}\left\|\mathbf{\Phi}+\mathbf{G}\mathbf{U}_k\mathbf{F}_i\right\|_F^2-\left[1-K\Gamma_{\mathrm{req}_{i,k}}^{\mathrm{EVE}}\right]\left[\mathrm{Tr}\left(\left(\mathbf{\Phi}^{(j)}\right)^H\mathbf{\Phi}\right)-\frac{1}{2}\left\|\mathbf{\Phi}^{(j)}\right\|_F^2\right]\\
&+\Gamma_{\mathrm{req}_{i,k}}^{\mathrm{EVE}}\sum_{r\in\mathscr{K}\setminus\{k\}}\left[\mathrm{Tr}\left(\left(\mathbf{F}_i^H\mathbf{G}^H\mathbf{G}\mathbf{U}_r^{(j)}\mathbf{F}_i\right)^H\mathbf{U}_r\right)-\frac{1}{2}\left\|\mathbf{G}\mathbf{U}_r^{(j)}\mathbf{F}_i\right\|_F^2\right]-\mathrm{Tr}\left(\left(\mathbf{F}_i^H\mathbf{G}^H\mathbf{G}\mathbf{U}_k^{(j)}\mathbf{F}_i\right)^H\mathbf{U}_k\right)\\
&+\frac{1}{2}\left\|\mathbf{G}\mathbf{U}_k^{(j)}\mathbf{F}_i\right\|_F^2-\Gamma_{\mathrm{req}_{i,k}}^{\mathrm{EVE}}\left(\sum_{r\in\mathscr{K}\setminus\{k\}}\mathrm{Tr}\left(\mathbf{H}_i\mathbf{W}_r\right)+\mathrm{Tr}\left(\mathbf{H}_i\mathbf{Z}\right)+\sigma_d^2\mathrm{Tr}\left(\mathbf{\Phi}^H\mathbf{F}_i\mathbf{\Phi}\right)+\sigma_{n_k}^2\right)\\
&-\frac{\Gamma_{\mathrm{req}_{i,k}}^{\mathrm{EVE}}}{2}\sum_{r\in\mathscr{K}\setminus\{k\}}\left\|\mathbf{\Phi}+\mathbf{G}\mathbf{U}_r\mathbf{F}_i\right\|_F^2-\frac{\Gamma_{\mathrm{req}_{i,k}}^{\mathrm{EVE}}}{2}\left\|\mathbf{\Phi}+\mathbf{G}\mathbf{Q}\mathbf{F}_i\right\|_F^2+\Gamma_{\mathrm{req}_{i,k}}^{\mathrm{EVE}}\left[\mathrm{Tr}\left(\left(\mathbf{F}_i^H\mathbf{G}^H\mathbf{G}\mathbf{Q}^{(j)}\mathbf{F}_i\right)^H\mathbf{Q}\right)-\frac{1}{2}\left\|\mathbf{G}\mathbf{Q}^{(j)}\mathbf{F}_i\right\|_F^2\right]\\
&+\mathrm{Tr}\left(\mathbf{v}_i\mathbf{v}_i^H\begin{bmatrix}\mathbf{0} & \mathbf{U}_k^H-\Gamma_{\mathrm{req}_{i,k}}^{\mathrm{EVE}}\left(\sum_{r\in\mathscr{K}\setminus\{k\}}\mathbf{U}_r^H+\mathbf{Q}^H\right)\\ \mathbf{U}_k-\Gamma_{\mathrm{req}_{i,k}}^{\mathrm{EVE}}\left(\sum_{r\in\mathscr{K}\setminus\{k\}}\mathbf{U}_r+\mathbf{Q}\right) & \mathbf{0}\end{bmatrix}\right)\le 0,\forall i,\forall k, \qquad (4.24)
\end{aligned}$$

where $\mathbf{v}_i^H\in\mathbb{C}^{1\times(M+N_{\mathrm{T}})}$ is defined as $\mathbf{v}_i^H=\begin{bmatrix}\mathbf{f}_i^H & \mathbf{h}_i^H\end{bmatrix}$.

On the other hand, we note that constraint C7 and C9 are in the form of the difference of convex functions which are non-convex constraints. To address this issue, we construct the first-order Taylor approximation of $\mathrm{Tr}\left(\mathbf{W}_r\mathbf{G}^H\mathbf{G}\mathbf{W}_r^H\right)$ and $\mathrm{Tr}\left(\mathbf{Z}\mathbf{G}^H\mathbf{G}\mathbf{Z}^H\right)$. Specifically, we have

$$\mathrm{Tr}\left(\mathbf{W}_r\mathbf{G}^H\mathbf{G}\mathbf{W}_r^H\right)\ge-\left\|\mathbf{W}_r^{(j)}\mathbf{G}^H\right\|_F^2+2\mathrm{Tr}\left(\left(\mathbf{G}^H\mathbf{G}\mathbf{W}_r^{(j)}\right)^H\mathbf{W}_r\right), \qquad (4.25)$$

$$\mathrm{Tr}\left(\mathbf{Z}\mathbf{G}^H\mathbf{G}\mathbf{Z}^H\right)\ge-\left\|\mathbf{Z}^{(j)}\mathbf{G}^H\right\|_F^2+2\mathrm{Tr}\left(\left(\mathbf{G}^H\mathbf{G}\mathbf{Z}^{(j)}\right)^H\mathbf{Z}\right). \qquad (4.26)$$

Then, constraints C7 and C9 can be approximated by the following convex constraints:

$$\widehat{\mathrm{C7}}:\ \mathrm{Tr}\left(\mathbf{X}_r\right)+\left\|\mathbf{W}_r^{(j)}\mathbf{G}^H\right\|_F^2-2\mathrm{Tr}\left(\left(\mathbf{G}^H\mathbf{G}\mathbf{W}_r^{(j)}\right)^H\mathbf{W}_r\right)\le 0,\forall r\in\mathscr{K}, \qquad (4.27)$$

$$\widehat{\mathrm{C9}}:\ \mathrm{Tr}\left(\mathbf{M}\right)+\left\|\mathbf{Z}^{(j)}\mathbf{G}^H\right\|_F^2-2\mathrm{Tr}\left(\left(\mathbf{G}^H\mathbf{G}\mathbf{Z}^{(j)}\right)^H\mathbf{Z}\right)\le 0. \qquad (4.28)$$

4.3 Transformed Problems

In the (j+1)-th iteration of the IA-based algorithm, the first desirable system objective, i.e., the BS transmit power minimization problem in (4.4) is reformulated as follows

$$\begin{aligned}
P_1:\quad & f_1\left(\mathbf{W}_k,\mathbf{Z}\right)\triangleq\underset{\substack{\mathbf{\Phi},\mathbf{W}_k,\mathbf{Z},\mathbf{U}_k,\\ \mathbf{X}_k,\mathbf{Y}_k,\mathbf{Q},\mathbf{M},\mathbf{N}}}{\text{minimize}}\ \sum_{k\in\mathscr{K}}\mathrm{Tr}\left(\mathbf{W}_k\right)+\mathrm{Tr}\left(\mathbf{Z}\right) \qquad (4.29)\\
& \text{s.t.}\quad \widehat{\mathrm{C1}},\widehat{\mathrm{C2}},\mathrm{C3},\mathrm{C4},\mathrm{C5},\mathrm{C6},\widehat{\mathrm{C7}},\mathrm{C8},\widehat{\mathrm{C9}}.
\end{aligned}$$

We note that the only non-convexity of the optimization problem in (4.29) is the rank-one constraint C5.

On the other hand, for the second considered system objective, i.e., the active IRS amplification power minimization problem in (4.5), we handle the non-convex constraints C1 and C2 in the same way as we tackled them in Problem 1. Then, due to the non-convexity of the objective function, we further define a slack variable t and recast the optimization problem in (4.5) as follows:

$$\begin{aligned} & \underset{\substack{\mathbf{\Phi},\mathbf{W}_k,t,\mathbf{Z},\mathbf{U}_k,\\ \mathbf{X}_k,\mathbf{Y}_k,\mathbf{Q},\mathbf{M},\mathbf{N}}}{\text{minimize}} \quad t+\sigma_d^2\mathrm{Tr}\left(\mathbf{\Phi}\mathbf{\Phi}^H\right) \\ \text{s.t.} \quad & \widehat{\text{C1}},\widehat{\text{C2}},\text{C3},\text{C4},\text{C5},\text{C6},\widehat{\text{C7}},\text{C8},\widehat{\text{C9}}, \\ & \text{C10}:\sum_{k\in\mathscr{K}}\mathrm{Tr}\left(\mathbf{\Phi}\mathbf{G}\mathbf{W}_k\mathbf{G}^H\mathbf{\Phi}^H\right)\le t. \end{aligned} \tag{4.30}$$

To facilitate resource allocation algorithm design, we employ IA to approximate non-convex constraint C10 as follows

$$\begin{aligned} \widehat{\text{C10}}: \quad & \sum_{k\in\mathscr{K}}\left[\frac{1}{2}\left\|\mathbf{\Phi}+\mathbf{G}\mathbf{U}_k\right\|_F^2-\mathrm{Tr}\left(\left(\mathbf{G}^H\mathbf{G}\mathbf{U}_k^{(j)}\right)^H\mathbf{U}_k\right)+\frac{1}{2}\left\|\mathbf{G}\mathbf{U}_k^{(j)}\right\|_F^2\right] \\ & -K\left[\mathrm{Tr}\left(\left(\mathbf{\Phi}^{(j)}\right)^H\mathbf{\Phi}\right)-\frac{1}{2}\left\|\mathbf{\Phi}^{(j)}\right\|_F^2\right]+\sigma_d^2\mathrm{Tr}\left(\mathbf{\Phi}\mathbf{\Phi}^H\right)\le t \end{aligned} \tag{4.31}$$

Therefore, in the (j+1)-th iteration of the IA-based algorithm, we focus on the following optimization problem

$$\begin{aligned} P_2: \quad & \underset{\substack{\mathbf{\Phi},\mathbf{W}_k,t,\mathbf{Z},\mathbf{U}_k,\\ \mathbf{X}_k,\mathbf{Y}_k,\mathbf{Q},\mathbf{M},\mathbf{N}}}{\text{minimize}} \quad t+\sigma_d^2\mathrm{Tr}\left(\mathbf{\Phi}\mathbf{\Phi}^H\right) \\ \text{s.t.} \quad & \widehat{\text{C1}},\widehat{\text{C2}},\text{C3},\text{C4},\text{C5},\text{C6},\widehat{\text{C7}},\text{C8},\widehat{\text{C9}},\widehat{\text{C10}}. \end{aligned} \tag{4.32}$$

The transformed Problem 2 is non-convex due to the rank-one constraint C5.

Regarding the multi-objective optimization problem, we can equivalently reformulate it as follows

$$\begin{aligned} P_3: \quad & \underset{\substack{\mathbf{\Phi},\mathbf{W}_k,t,\mathbf{Z},\mathbf{U}_k,\\ \mathbf{X}_k,\mathbf{Y}_k,\mathbf{Q},\mathbf{M},\mathbf{N},\eta}}{\text{minimize}} \quad \eta \\ \text{s.t.} \quad & \widehat{\text{C1}},\widehat{\text{C2}},\text{C3},\text{C4},\text{C5},\text{C6},\widehat{\text{C7}},\text{C8},\widehat{\text{C9}},\widehat{\text{C10}}, \\ & \text{C11}:\lambda_i\left(L_i-L_i^*\right)\le\eta,\forall i\in\{1,2\}. \end{aligned} \tag{4.33}$$

where η is an auxiliary optimization variable, and constraint C11 is the epigraph representation [43] of (3.5). The remaining non-convex constraint in (4.33) is the rank-one

constraint C5. Solving such a rank-constrained problem is known to be NP-hard [44]. To overcome this obstacle, we remove rank-one constraint C5 by adopting SDR method. Then, the relaxed version of Problem 1, 2 and 3 are standard convex optimization problems and can be efficiently solved by convex program solvers such as CVX [45]. Next, taking the Problem 1 as an example, we verify the tightness of SDR by introducing the following theorem.

Theorem 1: If $\Gamma_{\text{req}_k} > 0$, the optimal beamforming matrix $\mathbf{W}_k^*$ obtained from (4.29) is always a rank-one matrix, i.e., $\text{Rank}(\mathbf{W}_k^*) = 1$.

Proof: By relaxing the rank-one constraint C5 in problem (4.29), the remaining problem is jointly convex with respect to the optimization variables and satisfies the Slater's constraint qualification. Therefore, strong duality holds and the Lagrangian function of the relaxed version of the optimization problem in (4.29) is given by

$$\begin{aligned}\mathscr{L} &= \sum_{k\in\mathscr{K}}\text{Tr}(\mathbf{W}_k) + \sum_{k\in\mathscr{K}}\delta_k\Gamma_{\text{req}_k}\sum_{r\in\mathscr{K}\setminus\{k\}}\text{Tr}\left(\mathbf{H}_k\mathbf{W}_r\right) - \sum_{k\in\mathscr{K}}\delta_k\text{Tr}\left(\mathbf{H}_k\mathbf{W}_k\right)\\ &+\sum_{i\in\mathscr{I}}\mu_i\sum_{k\in\mathscr{K}}\text{Tr}\left(\mathbf{H}_i\mathbf{W}_k\right) - \sum_{i\in\mathscr{I}}\mu_i\sum_{k\in\mathscr{K}}\Gamma^{\text{EVE}}_{\text{req}_{i,k}}\sum_{r\in\mathscr{K}\setminus\{k\}}\text{Tr}\left(\mathbf{H}_i\mathbf{W}_r\right) - \sum_{k\in\mathscr{K}}\text{Tr}\left(\boldsymbol{\Upsilon}_k\mathbf{W}_k\right)\\ &-\sum_{k\in\mathscr{K}}\text{Tr}\left(\boldsymbol{\Psi}_k\begin{bmatrix}\mathbf{X}_k & \mathbf{U}_k & \mathbf{W}_k\mathbf{G}^H\\ \mathbf{U}_k^H & \mathbf{Y}_k & \boldsymbol{\Phi}\\ \mathbf{G}\mathbf{W}_k^H & \boldsymbol{\Phi}^H & \mathbf{I}_M\end{bmatrix}\right) - 2\sum_{k\in\mathscr{K}}\tau_k\text{Tr}\left(\left(\mathbf{G}^H\mathbf{G}\mathbf{W}_k^{(j)}\right)^H\mathbf{W}_k\right) + \Lambda, \end{aligned} \tag{4.34}$$

where Λ denotes the terms which are irrelevant to $\mathbf{W}_k$. Variables δ_k, μ_i and τ_k are the Lagrange multipliers associated with constraints $\widehat{\text{C1}}$, $\widehat{\text{C2}}$ and C7, respectively. Matrices $\boldsymbol{\Upsilon}_k \succeq \mathbf{0}$ and $\boldsymbol{\Psi}_k \succeq \mathbf{0}$ are the Lagrange multipliers associated with the constraints C5 and $\widehat{\text{C6}}$ with respect to matrix $\mathbf{W}_k$, respectively. Therefore, the dual problem for the relaxed version of the optimization problem in (4.29) is given by

$$\underset{\substack{\boldsymbol{\Upsilon}_k,\boldsymbol{\Psi}_k\succeq\mathbf{0},\\ \delta_k,\mu_j,\tau_k\geq 0}}{\text{maximize}}\ \underset{\substack{\boldsymbol{\Phi},\mathbf{W}_k,\mathbf{Z},\mathbf{U}_k,\\ \mathbf{X}_k,\mathbf{Y}_k,\mathbf{Q},\mathbf{M},\mathbf{N}}}{\text{minimize}}\ \mathscr{L}(\boldsymbol{\Phi},\mathbf{W}_k,\mathbf{Z},\mathbf{U}_k,\mathbf{X}_k,\mathbf{Y}_k,\mathbf{Q},\mathbf{M},\mathbf{N},\boldsymbol{\Upsilon}_k,\boldsymbol{\Psi}_k,\delta_k,\mu_j,\tau_k). \tag{4.35}$$

Then, we follow a similar approach as proposed in [46]–[48], to investigate the structure of the optimal $\mathbf{W}_k^*$ by examining the Karush-Kuhn-Tucker (KKT) conditions for problem (4.29), which are given by:

$$\delta_k^*, \mu_j^*, \tau_k^* \geq 0, \boldsymbol{\Upsilon}_k^*, \boldsymbol{\Psi}_k^* \succeq \mathbf{0}, \tag{4.36}$$

$$\boldsymbol{\Upsilon}_k^*\mathbf{W}_k^* = \mathbf{0}, \tag{4.37}$$

$$\nabla_{\mathbf{W}_k^*}\mathscr{L} = \mathbf{0}, \tag{4.38}$$

where $\delta_k^*, \mu_j^*, \tau_k^* \geq 0$, $\boldsymbol{\Upsilon}_k^*$, and $\boldsymbol{\Psi}_k^*$ are the optimal Lagrange multipliers for dual problem (4.35), and $\nabla_{\mathbf{W}_k^*}\mathscr{L}$ denotes the gradient of Lagrangian function with respect to $\mathbf{W}_k^*$. With some basic algebraic operations, the KKT condition in (4.38) can be rewritten as

$$\boldsymbol{\Upsilon}_k^* = \mathbf{I}_{N_\mathrm{T}} - \boldsymbol{\Delta}_k^*, \tag{4.39}$$

where

$$\boldsymbol{\Delta}_k^* = \delta_k^*\mathbf{H}_k - \sum_{r\in\mathscr{K}\setminus\{k\}} \delta_r^*\Gamma_{\mathrm{req}_r}\mathbf{H}_r + 2\mathbf{D}_k^*\mathbf{G} + 2\tau_k^*\mathbf{G}^H\mathbf{G}\mathbf{W}_k^{(j)} - \sum_{i\in\mathscr{I}}\mu_i^*\mathbf{H}_i + \sum_{i\in\mathscr{I}}\mu_i^*\sum_{r\in\mathscr{K}\setminus\{k\}}\Gamma_{\mathrm{req}_{i,r}}^{\mathrm{EVE}}\mathbf{H}_i, \tag{4.40}$$

and $\mathbf{D}_k$ is obtained from $\boldsymbol{\Psi}_k$. The derivation of $\mathbf{D}_k$ is as follows:

We denote the constraint $\widehat{\mathrm{C6}}$ in (4.8) as $\boldsymbol{\Omega}_k \succeq \mathbf{0}, \forall k$, where $\boldsymbol{\Omega}_k \in \mathbb{C}^{(N_\mathrm{T}+2M)\times(N_\mathrm{T}+2M)}$. Since $\boldsymbol{\Psi}_k \succeq \mathbf{0}$ is the Lagrange multiplier matrix associated with the constraints $\widehat{\mathrm{C6}}$ with respect to $\mathbf{W}_k$, $\boldsymbol{\Psi}_k$ has the same dimensions as $\boldsymbol{\Omega}_k$. We note that all the elements of $\boldsymbol{\Omega}_k$ are matrices, and then we partition $\boldsymbol{\Psi}_k$ into multiple matrices. In particular, we have

$$\boldsymbol{\Psi}_k = \begin{bmatrix} \mathbf{A}_k & \mathbf{B}_k & \mathbf{D}_k \\ \mathbf{B}_k^H & \mathbf{C}_k & \mathbf{F}_k \\ \mathbf{D}_k^H & \mathbf{F}_k^H & \mathbf{E}_k \end{bmatrix}, \forall k, \tag{4.41}$$

where $\boldsymbol{\Psi}_k \in \mathbb{C}^{(N_\mathrm{T}+2M)\times(N_\mathrm{T}+2M)}$ and each matrix has the same dimension as the corresponding matrix in $\boldsymbol{\Omega}_k$. Then, we rewrite the term $\sum_{k\in\mathscr{K}} \mathrm{Tr}\left(\boldsymbol{\Psi}_k \begin{bmatrix} \mathbf{X}_k & \mathbf{U}_k & \mathbf{W}_k\mathbf{G}^H \\ \mathbf{U}_k^H & \mathbf{Y}_k & \boldsymbol{\Phi} \\ \mathbf{G}\mathbf{W}_k^H & \boldsymbol{\Phi}^H & \mathbf{I}_M \end{bmatrix}\right)$ in (4.34) as follows:

$$\begin{aligned}
&\sum_{k\in\mathscr{K}} \mathrm{Tr}\left(\begin{bmatrix} \mathbf{A}_k & \mathbf{B}_k & \mathbf{D}_k \\ \mathbf{B}_k^H & \mathbf{C}_k & \mathbf{F}_k \\ \mathbf{D}_k^H & \mathbf{F}_k^H & \mathbf{E}_k \end{bmatrix}\begin{bmatrix} \mathbf{X}_k & \mathbf{U}_k & \mathbf{W}_k\mathbf{G}^H \\ \mathbf{U}_k^H & \mathbf{Y}_k & \boldsymbol{\Phi} \\ \mathbf{G}\mathbf{W}_k^H & \boldsymbol{\Phi}^H & \mathbf{I}_M \end{bmatrix}\right) \\
&= \sum_{k\in\mathscr{K}} \mathrm{Tr}\left(\begin{bmatrix} \mathbf{A}_k\mathbf{X}_k + \mathbf{B}_k\mathbf{U}_k^H + \mathbf{D}_k\mathbf{G}\mathbf{W}_k^H & \cdots & \cdots \\ \cdots & \mathbf{B}_k^H\mathbf{U}_k + \mathbf{C}_k\mathbf{Y}_k + \mathbf{F}_k\boldsymbol{\Phi} & \cdots \\ \cdots & \cdots & \mathbf{D}_k^H\mathbf{W}_k\mathbf{G}^H + \mathbf{F}_k^H\boldsymbol{\Phi} + \mathbf{E}_k\mathbf{I}_M \end{bmatrix}\right) \\
&= \sum_{k\in\mathscr{K}} \mathrm{Tr}\left(\mathbf{A}_k\mathbf{X}_k + \mathbf{B}_k\mathbf{U}_k^H + \mathbf{D}_k\mathbf{G}\mathbf{W}_k^H + \mathbf{B}_k^H\mathbf{U}_k + \mathbf{C}_k\mathbf{Y}_k + \mathbf{F}_k\boldsymbol{\Phi} + \mathbf{D}_k^H\mathbf{W}_k\mathbf{G}^H + \mathbf{F}_k^H\boldsymbol{\Phi} + \mathbf{E}_k\mathbf{I}_M\right).
\end{aligned} \tag{4.42}$$

Then, we take the derivative of (4.42) with respect to $\mathbf{W}_k^*$ and the result is $2\mathbf{D}_k^*\mathbf{G}$.

Next, by unveiling the structure of matrix $\boldsymbol{\Upsilon}_k^*$, we show that the optimal $\mathbf{W}_k^*$ always satisfies $\mathrm{Rank}(\mathbf{W}_k^*) \leq 1$. We first reveal that $\boldsymbol{\Delta}_k^*$ is a positive semidefinite matrix by

Algorithm 1 Inner Approximation Algorithm

1: Take Problem 1 as an example, set initial point $\mathbf{W}_k^{(j)}$, $\mathbf{\Phi}^{(j)}$, $\mathbf{Z}^{(j)}$, $\mathbf{U}_k^{(j)}$, $\mathbf{X}_k^{(j)}$, $\mathbf{Y}_k^{(j)}$, $\mathbf{Q}^{(j)}$, $\mathbf{M}^{(j)}$ and $\mathbf{N}^{(j)}$, iteration index $j=1$, and error tolerance $0 \leq \varepsilon \leq 1$;
2: **repeat**
3: For given $\mathbf{W}_k^{(j)}$, $\mathbf{\Phi}^{(j)}$, $\mathbf{Z}^{(j)}$, $\mathbf{U}_k^{(j)}$, $\mathbf{X}_k^{(j)}$, $\mathbf{Y}_k^{(j)}$, $\mathbf{Q}^{(j)}$, $\mathbf{M}^{(j)}$ and $\mathbf{N}^{(j)}$, obtain the intermediate solution $\mathbf{W}_k^{(j+1)}$, $\mathbf{\Phi}^{(j+1)}$, $\mathbf{Z}^{(j+1)}$, $\mathbf{U}_k^{(j+1)}$, $\mathbf{X}_k^{(j+1)}$, $\mathbf{Y}_k^{(j+1)}$, $\mathbf{Q}^{(j+1)}$, $\mathbf{M}^{(j+1)}$ and $\mathbf{N}^{(j+1)}$ by solving the rank constraint-relaxed version of problem (4.29);
4: Set $j=j+1$;
5: **until** $\frac{f(\mathbf{W}_k^{(j-1)},\mathbf{Z}^{(j-1)})-f(\mathbf{W}_k^{(j)},\mathbf{Z}^{(j)})}{f(\mathbf{W}_k^{(j)},\mathbf{Z}^{(j)})} \leq \varepsilon$.

contradiction. Specifically, if $\mathbf{\Delta}_k^*$ is a negative definite matrix, according to (4.39), then $\mathbf{\Upsilon}_k^*$ must be a full-rank positive definite matrix. Considering the KKT condition in (4.37), it implies that $\mathbf{W}_k^* = \mathbf{0}$, which cannot be an optimal solution for $\Gamma_{\text{req}_k} > 0$. Hence, $\mathbf{\Delta}_k^*$ must be a positive semidefinite matrix. Since the matrix $\mathbf{\Upsilon}_k^*$ is also positive semidefinite, we have

$$1 \geq \nu_{\mathbf{\Delta}_k^*}^{\max} \geq 0 \tag{4.43}$$

where $1 \geq \nu_{\mathbf{\Delta}_k^*}^{\max} \geq 0$ denotes the maximum eigenvalue of matrix $\mathbf{\Delta}_k^*$. However, due to the randomness of the channels, the case where multiple eigenvalues have the same value of $\nu_{\mathbf{\Delta}_k^*}^{\max}$ occurs with probability zero. For the case where $\nu_{\mathbf{\Delta}_k^*}^{\max} > 1$, according to (4.39), the obtained matrix $\mathbf{\Upsilon}_k^*$ is not positive semidefinite, which contradicts the KKT condition in (4.36). On the other hand, if $\nu_{\mathbf{\Delta}_k^*}^{\max} \leq 1$, then the $\mathbf{\Upsilon}_k^*$ is a positive semidefinite matrix with $\text{Rank}(\mathbf{\Upsilon}_k^*) \geq N_{\text{T}} - 1$. Considering (4.37), this leads to $\text{Rank}(\mathbf{W}_k^*) \leq 1$, which completes the proof. □

Note that the relaxed version of (4.29) and (4.32) are convex optimization problems, and the proposed IA-based algorithm for solving them is summarized in **Algorithm 1**. According to [49, Theorem 1], the objective functions in (4.29) and (4.32) are non-increasing in each iteration and the proposed algorithm is guaranteed to converge to the locally optimal solutions of (3.3) and (3.4) in polynomial time. The per iteration computational complexity of **Algorithm 1** is given by $\mathcal{O}(\log(1/\varepsilon)((3(K+I)+1)^3+(3(K+I)+1)^2N_{\text{T}}^2)+(3(K+I)+1)N_{\text{T}}^3+(2(K+I)+1)^3+(2(K+I)+1)^2M^2+(2(K+I)+1)M^3))$, where $\mathcal{O}(\cdot)$ is the big-O notation and ε is the convergence tolerance of **Algorithm 1**.

Chapter 5

Simulation Results

In this chapter, we evaluate the system performance of the proposed resource allocation scheme via simulations. In particular, we assume that the BS serves one sector of a cell with a radius of $R = 50$ m and the active IRS with M elements is deployed at the edge of the cell. The $K = 3$ users and $I = 2$ potential eavesdroppers are randomly and uniformly distributed in the sector. The channel matrix $\mathbf{G}$ between the BS and active IRS is modeled as

$$\mathbf{G} = \sqrt{\iota_0 R^{\alpha}}\left(\sqrt{\frac{\kappa}{1+\kappa}}\mathbf{G}_{\mathrm{L}} + \sqrt{\frac{1}{1+\kappa}}\mathbf{G}_{\mathrm{N}}\right), \tag{5.1}$$

where $\iota_0 = (\frac{\lambda_c}{4\pi})^2$ is a constant with λ_c being the wavelength of the carrier frequency and α is the path loss exponent. The small-scale fading is assumed to be Rician fading with Rician factor $\kappa = 3$ dB. $\mathbf{G}_{\mathrm{L}}$ and $\mathbf{G}_{\mathrm{N}}$ are the line-of-sight (LoS) and non-LoS components, respectively. The LoS component is the product of the receive and transmit array response vectors while the non-LoS component is modeled by Rayleigh fading. The channel vectors between the active IRS and all users and between the active IRS and the eavesdroppers are generated in a similar manner as $\mathbf{G}$. In addition, the path loss exponents for the direct links and the reflection links between BS and users and between BS and eavesdroppers are α_d and α_r, respectively. For the ease of presentation, we assume that the minimum required SINRs of all users and eavesdroppers are identical, i.e., $\Gamma_{\mathrm{req}_k} = \Gamma_{\mathrm{req}}$ and $\Gamma_{i,k}^{\mathrm{EVE}} = \Gamma_{\mathrm{req}}^{\mathrm{EVE}}$. The important system parameters adopted in our simulations are listed in Table.5.1.

To show the effectiveness of the proposed scheme, we also consider three baseline schemes for comparison. For baseline scheme 1, we adopt simple design choices without performing iterative optimization. In particular, we adopt Maximum Ratio Transmission (MRT) for transmit beamforming, apply AN injection at the BS , and implement the IRS with random phases. For baseline scheme 2, we optimize the beamforming vectors $\mathbf{w}_k$ for minimization of the power consumption and apply an isotropic radiation pattern for AN injection at the BS. For baseline scheme 3, to further investigate the per-

Table 5.1: System Parameters in Simulations

Carrier center frequency	f_c	2.4 GHz
Number of antenna elements	N_{T}	4
Path loss exponent for direct links	α_{d}	3.5
Path loss exponent for reflection links	α_{r}	2.3
Noise power at users	σ_k^2	-90 dBm
Dynamic noise power	σ_d^2	-100 dBm [21]
Error tolerance factor	ε	0.001

formance of active IRS, we consider a conventional IRS-assisted system in which the IRS elements just passively reflect the incident signals without amplification. In particular, we optimize the beamforming vectors $\mathbf{w}_k$ and apply AN injection at the BS.

5.1 Trade-off between BS Transmit Power and Active IRS Amplification Power

In Fig.5.1, we study the trade-off between the BS transmit power and the active IRS amplification power for different QoS requirements of users. The trade-off region is obtained by solving (4.33) for different $0 \leq \lambda_i \leq 1, \forall i \in \{1,2\}$, i.e., the λ_i are varied uniformly using a step size of 0.025 subject to $\sum_i \lambda_i = 1$. It can be observed from Fig.5.1 that the average active IRS amplification power is a monotonically decreasing function with respect to the average BS transmit power. In other words, minimizing the the average active IRS amplification power consumption leads to a higher power consumption in the BS and vice versa. This result confirms that the minimization of the total BS transmit power and the active IRS amplification power are conflicting objectives. For a power-limited communication system, there is a trade-off in resource allocation between BS and active IRS. For the case of $\Gamma_k = 4$ dB, 8.8 dB in BS transmit power can be saved by increasing the average active IRS amplification power by 6.8 dB. Moreover, Fig.5.1 also indicates that the BS and the active IRS have to consume more power to satisfy a higher SINR requirement of users. Furthermore, each curve corresponds to a set of resource allocation policies. Thus, the operator can select a proper resource allocation policy from the set of available policies based on the actual requirements.

We can also observe from Fig.5.1 that the proposed scheme yields substantial power savings compared to the two baseline schemes. In particular, for baseline scheme 1, both the BS and the active IRS cannot fully exploit the Degrees of Freedom (DoFs) available for resource allocation due to the fixed MRT beamforming policy and the randomly generated IRS phase shifts, respectively. As for baseline scheme 2, the performance loss

compared to the proposed scheme is mainly due to the fixed AN design. This highlights the effectiveness of the proposed scheme for jointly optimizing the transmit beamforming vectors, AN covariance matrix, and the active IRS elements.

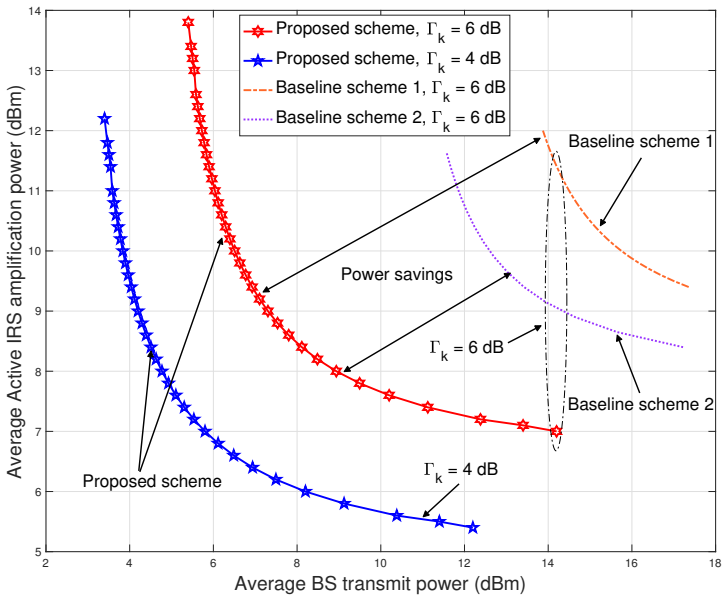

Figure 5.1: Trade-off between average BS transmit power (dBm) and average active IRS amplification power (dBm) for different resource allocation schemes with $K = 3$, $I = 2$, $N_{\mathrm{T}} = 6$, $M = 10$, $\alpha_d = 3.5$, $\alpha_r = 2.3$, $R = 50$ m and $\Gamma_{\mathrm{req}}^{\mathrm{EVE}} = 2$ dB.

5.2 BS Transmit Power vs. Minimum Required SINR

In Fig.5.2, we investigate the average BS transmit power versus the minimum required SINR at the users, Γ_{req_k}. We select the resource allocation policy with $\lambda_1 = 0.7$ and $\lambda_2 = 0.3$ which indicates that the system operator attaches a higher priority to BS transmit power minimization. As can be observed from Fig.5.2 that, the average BS transmit power of all the schemes monotonically increases with Γ_{req_k}. This is due to the fact that, as Γ_{req_k} increases, the BS has to transmit with a higher power to satisfy the QoS of the users. Moreover, we observe that the proposed scheme consumes less transmit power compared to that of the two baseline schemes. In particular, the significant power savings is achieved by the joint optimization of the transmit beamforming vectors, AN covariance matrix, and the active IRS elements. On the other hand, increasing the number of transmit antennas and IRS elements further saves the BS transmit power. This is due to the fact that the extra degrees freedom offered by the additional anten-

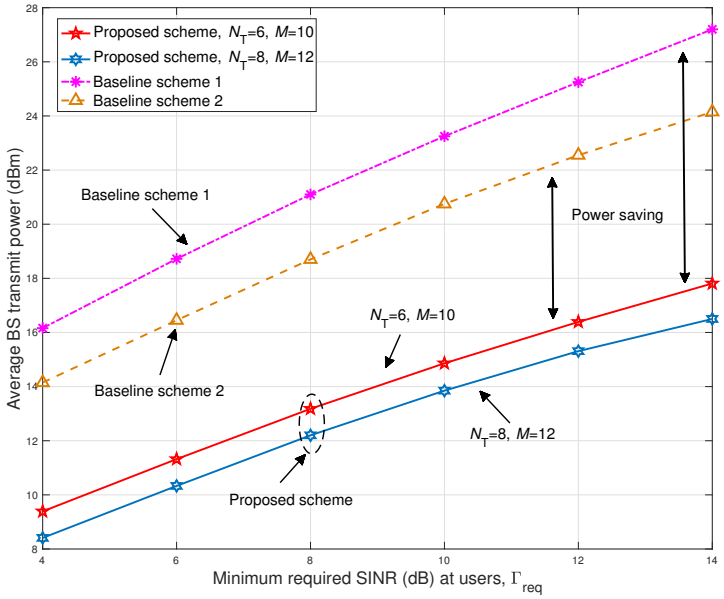

Figure 5.2: Average BS transmit power (dBm) vs. minimum required SINR of the users different resource allocation schemes with $K = 3$, $I = 2$, $N_{\mathrm{T}} = 6$, $M = 10$, $\alpha_d = 3.5$, $\alpha_r = 2.3$, $R = 50$ m and $\Gamma_{\mathrm{req}}^{\mathrm{EVE}} = 2$ dB.

nas and active IRS elements facilitate a more power efficient resource allocation which yields transmit power savings. On the contrary, the two baseline schemes require huge power consumption. Specifically, for baseline scheme 1, the fixed MRT beamforming is unable to fully exploit the DoFs introduced by the active IRS elements. In fact, the MRT strategy fails to mitigate multiuser interference, resulting in poor performance. As for baseline scheme 2, due to the the fixed AN design, the BS has to consume more power to satisfy the QoS of all the users and guarantee the secure communication.

5.3 Energy Efficiency vs. Number of IRS Elements

IRSs are recognized as energy-efficient devices for improving communication performance. To further investigate the performance of active IRSs, we adopt the energy efficiency (bits/J/Hz) as the performance metric which is defined as [50, Eq.(19)]

$$\xi = \frac{\sum\limits_{k\in\mathscr{K}} \log_2\left(1+\Gamma_k\right)}{\frac{1}{\eta}\left(\sum\limits_{k\in\mathscr{K}} \|\mathbf{w}_k\|^2 + \mathrm{Tr}\left(\mathbf{Z}\right)\right) + N_{\mathrm{T}}P_{\mathrm{T}} + P_{\mathrm{C}} + MP_{\mathrm{I}} + \frac{1}{\eta}P_{\mathrm{A}}}, \tag{5.2}$$

where $\eta = 0.5$ is the power amplifier efficiency, $P_{\mathrm{T}} = 100$mW is the circuit power that maintains one BS antenna element operational, $P_{\mathrm{C}} = 85$mW is the static circuit power of

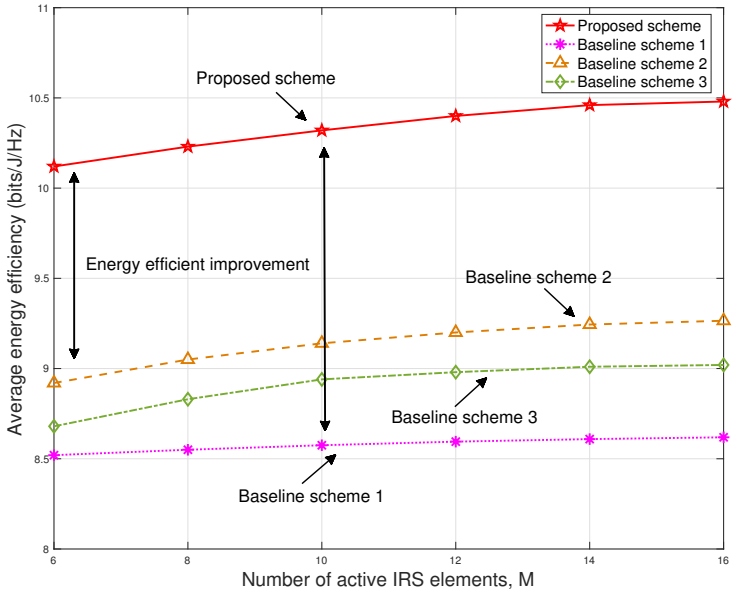

Figure 5.3: Average energy efficiency vs. the number of active IRS elements for different resource allocation schemes with $K = 3$, $I = 2$, $N_{\mathrm{T}} = 6$, $\alpha_d = 2.9$, $\alpha_r = 2.3$, $R = 50$ m, $\Gamma_{\mathrm{req}} = 10$ dB and $\Gamma_{\mathrm{req}}^{\mathrm{EVE}} = 2$ dB.

the BS, $P_{\mathrm{I}} = 2$mW is the circuit power required to support one IRS element, and P_{A} is the power allocated to the active IRS. Fig.5.3 illustrates the average energy efficiency versus the number of active IRS elements for a scenario where the direct links are slightly shadowed ($\alpha_d = 2.9$). As can be observed from Fig.5.3, increasing the number of active IRS elements leads to an improvement of the energy efficiency for all schemes. In particular, due to the low-power consumption of IRS phase shifters, deploying more IRS elements does not significantly increase the operational power of the IRS. Moreover, additional IRS elements introduce extra DoFs that can be exploited to create a more favorable propagation environment which allows a further reduction of the transmit power. On the other hand, we observe that the proposed scheme outperforms the three baseline schemes. This is because the proposed scheme is able to fully exploit the extra DoFs by jointly optimizing both the beamforming vectors, the AN covariance matrix and the active IRS elements which effectively facilitates more accurate beamforming and saves more transmit power. For the baseline scheme 1, the fixed MRT beamforming policy is unable to fully exploit the extra DoFs introduced by additional IRS elements, which leads to an insignificant improvement in energy efficiency. As for the baseline scheme 3, deploying passive IRS can not effectively enhance performance due to the double path loss effect, especially when the direct links are not weak. In contrast, employing the active IRS can simultaneously adjust the phase and the amplitude of the reflected

signal to combat the double path loss effect. This observation strongly encourages the application of active IRSs to further improve the system performance.

Chapter 6

Conclusion

In this thesis, we investigated resource allocation algorithm design for multiuser MISO wireless communication systems. To overcome the "double path loss" effect introduced by conventional IRSs, we deployed an active IRS in the considered system to improve the system performance. Different from the conventional IRS that just passively reflects signals without amplification, the key feature of active IRSis the capability of actively reflecting signals with amplification at the expense of additional power consumption. To guarantee communication security, we applied AN injection at BS to deliberately degrade the channels of the eavesdroppers. However, the total available power of communication systems is limited. We need to smartly allocate power to the BS transmit power and the IRS amplification power while satisfying the QoS requirements of the users. To this end, we exploited a multi-objective optimization framework to study the trade-off in resource allocation between two conflicting yet desirable design objectives, i.e., BS transmit power minimization and active IRS amplification power minimization. We adopted weighted Tchebycheff method to formulate the multi-objective optimization problem. Although the proposed multi-objective optimization problem is non-convex, we solve it optimally by employing SDR and IA.

Simulation results not only unveiled the trade-off in resource allocation between the BS and the active IRS, but also showed that the proposed scheme achieves considerable power savings compared to the baseline schemes. Moreover, our results revealed that active IRSs are a promising means to overcome the double path loss effect in conventional IRS-assisted communication systems and motivates the application of active IRSs to further improve the system performance.

Bibliography

[1] Federico Boccardi, Robert W. Heath, Angel Lozano, Thomas L. Marzetta, and Petar Popovski. Five disruptive technology directions for 5G. *IEEE Communications Magazine*, 52(2):74–80, 2014.

[2] Ertugrul Basar, Marco Di Renzo, Julien De Rosny, Merouane Debbah, Mohamed-Slim Alouini, and Rui Zhang. Wireless communications through reconfigurable intelligent surfaces. *IEEE access*, 7:116753–116773, 2019.

[3] Marco Di Renzo, Alessio Zappone, Merouane Debbah, Mohamed-Slim Alouini, Chau Yuen, Julien de Rosny, and Sergei Tretyakov. Smart Radio Environments Empowered by Reconfigurable Intelligent Surfaces: How It Works, State of Research, and The Road Ahead. *IEEE Journal on Selected Areas in Communications*, 38(11):2450–2525, 2020.

[4] Chongwen Huang, Sha Hu, George C Alexandropoulos, Alessio Zappone, Chau Yuen, Rui Zhang, Marco Di Renzo, and Merouane Debbah. Holographic MIMO surfaces for 6G wireless networks: Opportunities, challenges, and trends. *IEEE Wireless Communications*, 27(5):118–125, 2020.

[5] Q. Wu and R. Zhang. Towards Smart and Reconfigurable Environment: Intelligent Reflecting Surface Aided Wireless Network. *IEEE Commun. Mag.*, 58(1):106–112, Jan. 2020.

[6] Yuanwei Liu, Xiao Liu, Xidong Mu, Tianwei Hou, Jiaqi Xu, Marco Di Renzo, and Naofal Al-Dhahir. Reconfigurable Intelligent Surfaces: Principles and Opportunities. *IEEE Communications Surveys Tutorials*, 23(3):1546–1577, 2021.

[7] T. Cui, M. Qi, X. Wan, J. Zhao, and Q. Cheng. Coding metamaterials, digital metamaterials and programmable metamaterials. *Light: Science & Applications*, 3(10):e218, 2014.

[8] Q. Wu and R. Zhang. Beamforming optimization for wireless network aided by intelligent reflecting surface with discrete phase shifts. *IEEE Trans. Commun.*, 2019.

[9] Xianghao Yu, Dongfang Xu, Derrick Wing Kwan Ng, and Robert Schober. IRS-assisted green communication systems: Provable convergence and robust optimization. *IEEE Transactions on Communications*, 2021.

[10] X. Yu, D. Xu, D. W. K. Ng, and R. Schober. Power-Efficient Resource Allocation for Multiuser MISO Systems via Intelligent Reflecting Surfaces. *accepted by IEEE Global Commun. Conf. (GLOBECOM), available at arXiv preprint arXiv:2005.06703*, 2020.

[11] Xianghao Yu, Dongfang Xu, Ying Sun, Derrick Wing Kwan Ng, and Robert Schober. Robust and secure wireless communications via intelligent reflecting surfaces. *IEEE Journal on Selected Areas in Communications*, 38(11):2637–2652, 2020.

[12] X. Yu, D. Xu, and R. Schober. MISO Wireless Communication Systems via Intelligent Reflecting Surfaces. In *Proc. IEEE Inter. Conf. Commun. in China (ICCC)*, Changchun, China, Aug. 2019.

[13] Dongfang Xu, Xianghao Yu, Vahid Jamali, Derrick Wing Kwan Ng, and Robert Schober. Resource allocation for large IRS-assisted SWIPT systems with non-linear energy harvesting model. In *2021 IEEE Wireless Communications and Networking Conference (WCNC)*, pages 1–7. IEEE, 2021.

[14] Linglong Dai, Bichai Wang, Min Wang, Xue Yang, Jingbo Tan, Shuangkaisheng Bi, Shenheng Xu, Fan Yang, Zhi Chen, Marco Di Renzo, et al. Reconfigurable intelligent surface-based wireless communications: Antenna design, prototyping, and experimental results. *IEEE Access*, 8:45913–45923, 2020.

[15] Chongwen Huang, Ronghong Mo, and Chau Yuen. Reconfigurable intelligent surface assisted multiuser MISO systems exploiting deep reinforcement learning. *IEEE Journal on Selected Areas in Communications*, 38(8):1839–1850, 2020.

[16] Peilan Wang, Jun Fang, Xiaojun Yuan, Zhi Chen, and Hongbin Li. Intelligent reflecting surface-assisted millimeter wave communications: Joint active and passive precoding design. *IEEE Transactions on Vehicular Technology*, 69(12):14960–14973, 2020.

[17] Chongwen Huang, Alessio Zappone, George C Alexandropoulos, Mérouane Debbah, and Chau Yuen. Reconfigurable intelligent surfaces for energy efficiency in wireless communication. *IEEE Transactions on Wireless Communications*, 18(8):4157–4170, 2019.

[18] M. Najafi, V. Jamali, R. Schober, and H. V. Poor. Physics-based Modeling and Scalable Optimization of Large Intelligent Reflecting Surfaces. *under revision in IEEE Trans. Commun., available at arXiv preprint arXiv:2004.12957*, 2020.

[19] Dongfang Xu, Vahid Jamali, Xianghao Yu, Derrick Wing Kwan Ng, and Robert Schober. Optimal Resource Allocation Design for Large IRS-Assisted SWIPT Systems: A Scalable Optimization Framework. *arXiv preprint arXiv:2104.03346*, 2021.

[20] Q. Wu and R. Zhang. Intelligent Reflecting Surface Enhanced Wireless Network via Joint Active and Passive Beamforming. *IEEE Trans. Wireless Commun.*, 18(11):5394–5409, Nov. 2019.

[21] Zijian Zhang, Linglong Dai, Xibi Chen, Changhao Liu, Fan Yang, Robert Schober, and H Vincent Poor. Active RIS vs. passive RIS: Which will prevail in 6G? *arXiv preprint arXiv:2103.15154*, 2021.

[22] Dongfang Xu, Xianghao Yu, Derrick Wing Kwan Ng, and Robert Schober. Resource allocation for active IRS-assisted multiuser communication systems. *arXiv preprint arXiv:2108.13033*, 2021.

[23] Yan Sun, Derrick Wing Kwan Ng, and Robert Schober. Multi-Objective Optimization for Power Efficient Full-Duplex Wireless Communication Systems. In *2015 IEEE Global Communications Conference (GLOBECOM)*, pages 1–6, 2015.

[24] Yan Sun, Derrick Wing Kwan Ng, Jun Zhu, and Robert Schober. Robust and secure resource allocation for full-duplex MISO multicarrier NOMA systems. *IEEE Trans. Commun.*, 66(9):4119–4137, 2018.

[25] Bruce Schneier. Cryptographic design vulnerabilities. *Computer*, 31(9):29–33, 1998.

[26] Y. Wu, R. Schober, D. W. K. Ng, C. Xiao, and G. Caire. Secure Massive MIMO Transmission With an Active Eavesdropper. *IEEE Transactions on Information Theory*, 62(7):3880–3900, 2016.

[27] Meng Zhang and Yuan Liu. Energy harvesting for physical-layer security in OFDMA networks. *IEEE Transactions on Information Forensics and Security*, 11(1):154–162, 2015.

[28] Jun Zhu, Robert Schober, and Vijay K Bhargava. Linear precoding of data and artificial noise in secure massive MIMO systems. *IEEE Transactions on Wireless Communications*, 15(3):2245–2261, 2015.

[29] Yan Sun, Derrick Wing Kwan Ng, Jun Zhu, and Robert Schober. Multi-objective optimization for robust power efficient and secure full-duplex wireless communication systems. *IEEE Transactions on Wireless Communications*, 15(8):5511–5526, 2016.

[30] Derrick Wing Kwan Ng, Ernest S Lo, and Robert Schober. Robust beamforming for secure communication in systems with wireless information and power transfer. *IEEE Transactions on Wireless Communications*, 13(8):4599–4615, 2014.

[31] Meng Zhang, Yuan Liu, and Rui Zhang. Artificial noise aided secrecy information and power transfer in OFDMA systems. *IEEE Transactions on Wireless Communications*, 15(4):3085–3096, 2016.

[32] Satashu Goel and Rohit Negi. Guaranteeing secrecy using artificial noise. *IEEE transactions on wireless communications*, 7(6):2180–2189, 2008.

[33] Xiangyun Zhou and Matthew R McKay. Secure transmission with artificial noise over fading channels: Achievable rate and optimal power allocation. *IEEE Transactions on Vehicular Technology*, 59(8):3831–3842, 2010.

[34] Jing Huang and A Lee Swindlehurst. Robust secure transmission in MISO channels based on worst-case optimization. *IEEE Transactions on Signal Processing*, 60(4):1696–1707, 2011.

[35] Hui-Ming Wang, Chao Wang, and Derrick Wing Kwan Ng. Artificial noise assisted secure transmission under training and feedback. *IEEE Transactions on Signal Processing*, 63(23):6285–6298, 2015.

[36] Q. Li and W. K. Ma. Spatially selective artificial-noise aided transmit optimization for MISO multi-eves secrecy rate maximization. *IEEE Transactions on Signal Processing*, 61(10):2704–2717, 2013.

[37] Changsheng You and Rui Zhang. Wireless Communication Aided by Intelligent Reflecting Surface: Active or Passive? *IEEE Wireless Communications Letters*, 10(12):2659–2663, 2021.

[38] Jean-François Bousquet, Sebastian Magierowski, and Geoffrey G. Messier. A 4-GHz Active Scatterer in 130-nm CMOS for Phase Sweep Amplify-and-Forward. *IEEE Transactions on Circuits and Systems I: Regular Papers*, 59(3):529–540, 2012.

[39] R Timothy Marler and Jasbir S Arora. Survey of multi-objective optimization methods for engineering. *Structural and multidisciplinary optimization*, 26(6):369–395, 2004.

[40] Derrick Wing Kwan Ng, Ernest S Lo, and Robert Schober. Multiobjective resource allocation for secure communication in cognitive radio networks with wireless information and power transfer. *IEEE transactions on vehicular technology*, 65(5):3166–3184, 2015.

[41] Umar Rashid, Hoang Duong Tuan, Ha Hoang Kha, and Ha H Nguyen. Joint optimization of source precoding and relay beamforming in wireless MIMO relay networks. *IEEE Transactions on communications*, 62(2):488–499, 2014.

[42] Kemin Zhou and John Comstock Doyle. *Essentials of robust control*, volume 104. Prentice hall Upper Saddle River, NJ, 1998.

[43] S. Boyd and L. Vandenberghe. *Convex optimization*. Cambridge university press, 2004.

[44] Bernd Gärtner and Jiri Matousek. *Approximation algorithms and semidefinite programming*. Springer Science & Business Media, 2012.

[45] M. Grant and S. Boyd. CVX: Matlab software for disciplined convex programming, version 2.1. *Available at http://cvxr.com/cvx*, Mar. 2017.

[46] D. Xu, X. Yu, Y. Sun, D. W. K. Ng, and R. Schober. Resource allocation for IRS-assisted full-duplex cognitive radio systems. *IEEE Trans. Commun.*, to appear, 2020.

[47] E. Boshkovska, D. W. K. Ng, N. Zlatanov, A. Koelpin, and R. Schober. Robust resource allocation for MIMO wireless powered communication networks based on a non-linear EH model. *IEEE Transactions on Communications*, 2017.

[48] Y. Sun, D. W. K. Ng, and R. Schober. Resource Allocation for Secure Full-Duplex Radio Systems. In *WSA 2017; 21th International ITG Workshop on Smart Antennas; Proceedings of VDE*, pages 1–6, 2017.

[49] Barry R Marks and Gordon P Wright. A general inner approximation algorithm for nonconvex mathematical programs. *Operations research*, 26(4):681–683, 1978.

[50] Xianghao Yu, Dongfang Xu, Derrick Wing Kwan Ng, and Robert Schober. Power-Efficient Resource Allocation for Multiuser MISO Systems via Intelligent Reflecting Surfaces. In *GLOBECOM 2020 - 2020 IEEE Global Communications Conference*, pages 1–6, 2020.